Bioclim

2003

Modelling Sequential Biosphere Systems under Climate Change for Radioactive Waste Disposal

EC-CONTRACT : FIKW-CT-2000-00024

Deliverable D6a :

Regional climatic characteristics for the European sites at specific times : the dynamical downscaling.

Work package 2: Simulation of the future evolution of the biosphere system using the hierarchical strategy

Foreword

The BIOCLIM project on modelling sequential BIOsphere systems under CLIMate change for radioactive waste disposal is part of the EURATOM fifth European framework programme. The project was launched in October 2000 for a three-year period. The project aims at providing a scientific basis and practical methodology for assessing the possible long term impacts on the safety of radioactive waste repositories in deep formations due to climate and environmental change. Five work packages have been identified to fulfil the project objectives:

Work package 1 will consolidate the needs of the European agencies of the consortium and summarise how environmental change has been treated to date in performance assessments.

Work packages 2 and 3 will develop two innovative and complementary strategies for representing time series of long term climate change using different methods to analyse extreme climate conditions (the hierarchical strategy) and a continuous climate simulation over more than the next glacial-interglacial cycle (the integrated strategy).

Work package 4 will explore and evaluate the potential effects of climate change on the nature of the biosphere systems.

Work package 5 will disseminate information on the results obtained from the three year project among the international community for further use.

The project brings together a number of representatives from both European radioactive waste management organisations which have national responsibilities for the safe disposal of radioactive waste, either as disposers or regulators, and several highly experienced climate research teams, which are listed below.

- Agence Nationale pour la Gestion des Déchets Radioactifs (Andra), France – **J. Brulhet, D.Texier**
- Commissariat à l'Energie Atomique/ Laboratoire des Sciences du Climat et de l'Environnement (CEA/LSCE) France – **N. de Noblet, D. Paillard, D.Lunt, P.Marbaix, M. Kageyama**
- United Kingdom Nirex Limited (NIREX), UK – **P. Degnan**
- Gesellschaft für Anlagen und Reaktorsicherheit mbH (GRS), Germany – **A. Becker**
- Empresa Nacional de Residuos Radioactivos S.A. (ENRESA), Spain – **A. Cortés**
- Centro de Investigaciones Energeticas, Medioambientales y Tecnologicas (CIEMAT), Spain – **A. Aguero, L. Lomba, P. Pinedo, F. Recreo, C. Ruiz,**
- Universidad Politecnica de Madrid Escuela Tecnica Superior de Ingenieros de Minas (UPM-ETSIMM), Spain – **M. Lucini , J.E. Ortiz, T. Torres**
- Nuclear Research Institute Rez, plc - Ustav jaderneho vyzkumu Rez a.s. (NRI), **Czech Republic – A. Laciok**
- Université catholique de Louvain/ Institut d'Astronomie et de Géophysique Georges Lemaître (UCL/ASTR), Belgium – **A. Berger, M.F. Loutre**
- The Environment Agency of England and Wales (EA), UK - **R. Yearsley, N. Reynard**
- University of East Anglia (UEA), UK – **C. Goodess, J. Palutikof**

BIOCLIM is supported by a Technical Secretariat provided by Enviros Consulting Ltd, with other technical support provided by Quintessa Ltd and Mike Thorne and Associates Ltd.

For this report, deliverable D6 of the BIOCLIM project, the main contributor UCL/ASTR. Public should be aware that BIOCLIM material is working material.

Content List

1. Introduction and objectives

The overall aim of BIOCLIM is to assess the possible long-term impacts due to climate change on the safety of radioactive waste repositories in deep formations. This aim is addressed through the following specific objectives:

- Development of practical and innovative strategies for representing sequential climatic changes to the geosphere-biosphere system for existing sites over central Europe, addressing the timescale of one million years, which is relevant to the geological disposal of radioactive waste.
- Exploration and evaluation of the potential effects of climate change on the nature of the biosphere systems used to assess the environmental impact.
- Dissemination of information on the new methodologies and the results obtained from the project among the international waste management community for use in performance assessments of potential or planned radioactive waste repositories.

The BIOCLIM project is designed to advance the state-of-the-art of biosphere modelling for use in Performance Assessments. Therefore, two strategies are developed for representing sequential climatic changes to geosphere-biosphere systems. The hierarchical strategy successively uses a hierarchy of climate models. These models vary from simple 2-D models, which simulate interactions between a few aspects of the Earth system at a rough surface resolution, through General Circulation Model (GCM) and vegetation model, which simulate in great detail the dynamics and physics of the atmosphere, ocean and biosphere, to regional models, which focus on the European regions and sites of interest. Moreover, rule-based and statistical downscaling procedures are also considered. Comparisons are provided in terms of climate and vegetation cover at the selected times and for the study regions. The integrated strategy consists of using integrated climate models, representing all the physical mechanisms important for long-term continuous climate variations, to simulate the climate evolution over many millennia. These results are then interpreted in terms of regional climatic changes using rule-based and statistical downscaling approaches.

This deliverable, D6a, focuses on the hierarchical strategy, and in particular the MAR simulations. According to the hierarchical strategy developed in the BIOCLIM project to predict future climate, six BIOCLIM experiments were run with the MAR model. In addition to these experiments a baseline experiment, presenting the present-day climate simulated by MAR, was also undertaken. In the first step of the hierarchical strategy the LLN 2-D NH climate model simulated the gross features of the climate of the next 1 Myr [Ref.1]. Six snapshot experiments were selected from these results. In a second step a GCM and a biosphere model were used to simulate in more detail the climate of the selected time periods. These simulations were performed on a global scale [Ref.1]. The third step of the procedure is to derive the regional features of the climate at the same time periods. Therefore the results of the GCM are used as boundary conditions to force the regional climate model (MAR) for the six selected periods and the baseline simulation. The control simulation (baseline) corresponds to the regional climate simulated under present-day conditions, both insolation forcing and atmospheric CO_2 concentration. All the BIOCLIM simulations are compared to that baseline simulation. In addition, other comparisons will also be presented. Tableau 1 summarises the characteristics of these BIOCLIM experiments already presented in [Ref.1] and [Ref.2].

Name	Time (kyr AP)	CO_2 concentration (ppmv)	NH ice volume
Baseline	0	345	3.2
A	0	1100	3.2
B	0	550	0
C	67	550	0
D	67	345	0
E	67	345	3.2
F	178	280	17.4

Table 1: *Summary of the different snapshot experiments undergone under BIOCLIM project. The name of the simulations and their features are according to BIOCLIM Report D3 [Ref.2]. The time refers to the orbital parameters [Ref.3] that are used to compute the solar forcing. The NH ice volume corresponds to this variable in LLN 2-D NH in BIOCLIM Report D3 [Ref.2].*

This deliverable starts with a description of the MAR model and some adaptations for the specific use in BIOCLIM project. Previous experiments are also briefly reviewed. Most of the deliverable is devoted to the description of the future climate over western Europe as simulated in the MAR model. The regional model uses the IPSL_CM4_D simulated climate as boundary conditions. Simulations are started in October for 15 months. Results are presented for Winter (December-January-February: DJF) and Summer (June-July-August: JJA). They are intensively compared with the results from the IPSL_CM4_D model for the same seasons [Ref.1]. This is followed by a section focusing on the sites of interest.

All the figures of this deliverable are grouped together either as a separate file or at the back of this document.

2. The MAR model

2.1. - The model description

The MAR model Atmosphérique Régional) is a regional climate model designed to study the atmospheric component of the climate system and its interactions with the surface (soil and vegetation). It is adapted to domain sizes up to about 3000 km x 3000 km. The current version is a **hydrostatic** primitive-equation **atmospheric model**; the vertical coordinate is the normalised pressure (sigma-coordinate). The model includes detailed solar and infrared **radiation schemes** [Ref.4, Ref.5], close to schemes used in GCMs. It includes transmission and absorption by water vapour, clouds and trace gases, scattering. Clouds and precipitation are computed by a Kessler-type scheme, i.e. prognostic variables and conservation equations are included for four different hydrometeors, i.e. cloud droplets, cloud ice crystals, rain drops, and snowflakes [Ref.6]. Several **turbulence** closures of different complexity are available in the MAR model for the representation of the subgrid vertical fluxes. The simple 1.5 order scheme of Therry and Lacarrère [Ref.7] is used in the framework of this project. The first model layer is assumed to be a surface layer, in which the turbulent fluxes are assumed constant. Deep convection is the process by which moist convection instability can produce large vertical motions, which transports heat and moisture in the whole troposphere. Although the convective effects are sometimes the dominant atmospheric motion they cannot be resolved explicitly because of their small time and space-scale. Therefore a sophisticated convective parameterisation has been introduced [Ref.8]. The one dimensional land surface transfer model includes one vegetation layer and five soil layers (a soil skin layer and four sub-surface soil layers) (Surface Vegetation Atmosphere Transfert model, SVAT, [Ref.9]). The energy and water balances are included separately for the soil and the vegetation. The entire root zone is also taken into account. An effective leaf-area index accounts for the opening of leaves stomata. Plant transpiration and interception of rainwater by leaves are also represented. A snow model, including a parameterisation of the snow metamorphism processes in the snow pack, is also included. The snow albedo and the solar radiation extinction parameter are calculated from the simulated form and size of the snow grain. The surface albedo is also depending upon the presence of ice or meltwater at the surface of the ice sheet in case all snow has melted away. The meteorological information at the lateral boundaries of the domain is coming either from observation or from an atmospheric general circulation model. A pre-processing step is required to adapt the large-scale data prior to their use at the lateral boundary of the Modèle Atmosphérique Régional (MAR) because of both the enhanced resolution and the map projection. Lateral boundaries are treated by the standard relaxation scheme after adaptation of the large scale forcing to the model topography [Ref.10]. A general description of MAR can be found in Gallée and Schayes [Ref.11].

2.2. - Some adaptations

The MAR model needed to be adapted to the particular purpose of the BIOCLIM project.

The calendar used in MAR has been modified. It now comprises 12 months, each of them being 30 days long, instead of the actual calendar. This was undertaken to ensure consistency between MAR and the General Circulation Model (GCM).

Also the albedo, in particular the ocean albedo in the mid latitudes has been modified according to the values simulated by the GCM.

Different land-surface transfer models are available in the MAR model, for example:

- Forced-restored soil and humidity (Deardorff)
- A one-dimension land surface transfer model including one vegetation layer and five soil layers (SVAT)
- A more sophisticated model including vegetation, soil, snow and ice representation.

These different representations have advantages and disadvantages that must be tested in sensitivity experiments. Although the Deardorff model is not very sophisticated, it is routinely used and its drawbacks have been identified. On the other hand the more sophisticated representation still need to be validated, and adapted in the case of grid cells that are now ocean and that will become continent in a perturbed climate. Eventually the Deardorff model was used for BIOCLIM. The first simulations in the BIOCLIM configuration identified a cold bias, mostly localised over Southeast of the Alps. Further tests were performed to try to identify the reason for the cold bias. A parameterisation for the sub-grid height (effective rugosity) has been introduced. This parameterisation modifies the circulation in the low levels, the cold bias is indeed slightly reduced over the Southeast of the Alps but other biases, for example in the winds, appear or become larger. This parameterisation for the sub-grid height still needs to be refined.

2.3. - Application of MAR in previous experiments

The MAR model has already been tested on a variety of situations before this project. For example, within the CLIMOD project [Ref.12], the model was forced by the initial and lateral boundary conditions given by analyses of observation provided by the European Centre for Medium-Range Weather Forecasts (ECMWF). This simulation was performed over Western Europe and the simulation period was October 1986. This experiment demonstrated the ability of the MAR model to provide 3D simulations over at least one month [Ref.13]. Indeed the synoptic variability is correctly reproduced and there is no spurious trend in the variables at the time scale of one month and more.

The temperature and sea-level pressure are very well reproduced when pressure is low, and slightly less well reproduced when high pressure is present. In particular a cold temperature bias is often identified at the Southeast of the Alps. This cold bias of MAR is still under investigation. On the other hand the total amount, the geographic distribution and the day to day variability of the precipitation are also very satisfactorily simulated.

Different important issues were identified during these previous experiments.

- The horizontal filtering was adapted to the 50km resolution
- Some weaknesses in the Soil-vegetation model (SVAT) are still investigated during this project
- The cold temperature bias is still under examination.
- Some weaknesses in the Soil-vegetation model (SVAT) are still investigated during this project
- The cold temperature bias is still under examination.

The MAR model also proved its ability to simulate more extreme climates. The model was used over polar domains. The spatial evolution of the Antarctic katabatic winds in the area of Terra Nova Bay was studied [Ref.11]. Strong katabatic winds are simulated with a jet over Terra Nova Bay. The model initiated the mesocyclonic activity in the Ross Sea due to the katabatic circulation. Under fall climatic conditions, boundary layer fronts form due to the propagation of katabatic winds over the ocean. A surface pressure trough also forms and extends northeastward from Terra Nova Bay. [Ref.6]. The MAR model was also applied to study Greenland [Ref.14]. In particular, the ablation-refreezing process was analysed in depth for southern Greenland during summer 1991. The model was then forced at the lateral boundaries with European Centre for Medium-Range Weather

Forecasts re-analyses at a high horizontal resolution of 20 km.

The influence of the land use change in the southern part of Israel on local meteorological variables (e.g. diurnal amplitude of surface air temperature and wind speed, and increase of the October (early wet season) convective precipitation) were investigated [Ref.15].
A new wind gust estimate method has been tested [Ref.16] on two explosive cyclogenesis events that were satisfyingly simulated with the MAR mesoscale model nested in the ECMWF analysis. Daily maximum gusts are predicted with good accuracy, while the hourly temporal evolution of estimated gusts depends strongly on the accuracy of the meteorological fields generated by the model.
The MAR model has also proved its ability to simulate regional climate under perturbed greenhouse gases (GHG) conditions on the basis of an Ocean Atmosphere General Circulation Model (OAGCM) scenario experiment.

3. BIOCLIM experiments

3.1. - The MAR domain

The geographical domain is plotted on Figure 1. The domain size is 4200x3400 km and the grid size is 50x50 km. This large domain covers not only Western Europe but also a large part of the North Atlantic, North Africa and Eastern Europe.

This domain has been selected to cover the different regions of interest in BIOCLIM and the adjacent regions that could influence the climate of the regions of interest. Moreover, studies with other models suggest that this domain is probably large enough to allow the development of meso-scale circulation, which is not excessively constrained by the lateral boundaries. As far as topography is concerned it must be kept in mind that the altitude in each grid box is the mean altitude over the grid box. Namely, high peaks can be smoothed out because they do not extend over the whole grid box.

Moreover, a particular emphasis will be given to different regions in Europe. They are UK, France, Spain, Germany, and Czech Republic. Figure 2 gives the coordinates of these regions (NW and SE points of the box defining the region) and their position on the map.

3.2. - The baseline simulation

In this section, the MAR results from the 'baseline' simulation (present-day control experiment) are presented and compared to the GCM simulation [Ref.1]. An important point must be underlined here. The IPSL_CM4_D results presented in BIOCLIM Report D4/5 [Ref.1] are mean values over the last 30 years of the simulation. However the MAR simulations were forced by one single year, arbitrarily chosen. This particular year may be significantly different from the 30-yr average because of interannual variability. Therefore we decided to present, for the different variables, both the 30-yr average from the IPSL_CM4_D simulation and the particular year. Moreover the fields are also interpolated on the MAR grid, and the altitude effect is taken into account for the temperature. In addition to the MAR fields a composite variable (further called adjusted variable) is also displayed. The purpose of this variable is to extract from the MAR field the part of the signal that is produced by the IPSL_CM4_D model. This component is then added to the 30-yr average field from the IPSL_CM4_D model. This can be written as:

$$IPSL\_CM4\_D + (MAR\text{-}IPSL\_CM4\_D)$$

where *IPSL_CM4_D* represents the 30-yr average field, IPSL_CM4_D is the same field for the chosen year and MAR is the simulated field in the MAR model for the same year.

Surface temperature (Figure 3a). Here we present the 2m-high temperature. It is linearly extrapolated from the first two levels of the model. The Winter (DJF) temperature is exhibiting a clear gradient from the Southwest of Spain to the Northeast of the domain. There is no striking difference between the 30-yr average and the single year value. The chosen year is slightly warmer over the Mediterranean basin and Eastern Europe, and cooler in the Northwest of the domain. The regional model is enhancing the temperature gradient. The single year Summer (JJA) temperatures are warmer over the whole domain (Figure 4a). As far as most of the results will be compared to the reference simulation, the difference between the 30-yr average and the single year values could bias the anomalies. The regional model is responsible for a further cooling over the Pyrenees and the Alps. Values for the study areas are given in Tableau 2.

Total precipitation (Figure 3b). The 30-yr average Winter precipitation is showing large values over Portugal and the Northwest of Spain, as well as over the Bay of Biscay and the surrounding coasts. There is a minimum of precipitation over Central England. Precipitation decreases towards the East. The general pattern of Winter precipitation is very similar for the 30-yr average and the single year value. However the local differences *(IPSL_CM4_D-IPSL_CM4_D)* amount

to –0.7 mm.day^{-1} over the French Riviera and 0.7 mm.day^{-1} over Ireland. During Summer time, precipitation is very low over the Mediterranean basin; it is less that 0.5 mm.day^{-1} in south of Spain, south of Italy and Greece. Another minimum of precipitation is located over the Baltic countries. Precipitation is the largest in a region between 45 and 50°N in central Europe. The maximum of precipitation is smaller in the single year and located more eastward than in the 30-yr average. Namely, precipitation is larger in the single year than average over Belgium and lower than average over Slovenia (Figure 4b). Values for the study areas are given in Tableau 2.

Over the different regions of interest, MAR is showing colder temperatures in winter than IPSL_CM4_D, for the same year (Tableau 2). However this difference can be an artefact of the computation of this temperature. Indeed, none of the model is explicitly computing surface temperature. Rather temperature at the surface (as well as 2m-high temperature) is interpolated/extrapolated from temperature at higher levels. This procedure can induce large differences, especially during winter, when there is a large snow cover over the continents. In Summer most of the differences in temperature can be related with a better account of the elevation in MAR than in IPSL_CM4_D (due to a better resolution).

Baseline	MAR				IPSL_CM4_D			
	T. Surf.		Prec.		T. Surf.		Prec.	
	DJF	JJA	DJF	JJA	DJF	JJA	DJF	JJA
France	-3.5	20.7	3.86	1.84	1.8	19.8	3.66	2.87
Spain	4.0	21.1	4.25	0.16	9.5	20.1	3.66	0.64
C.England	-3.5	17.0	2.87	0.69	4.0	17.2	2.45	0.93
Czech R.	-11.1	20.2	1.73	0.92	-1.6	19.0	1.88	3.16
Germany	-9.8	22.0	2.22	0.96	-0.1	20.8	2.38	2.57

Table 2: *Baseline simulation. Surface temperature (°C) and precipitation (mm.day^{-1}) in DJF and JJA as simulated by the regional climate model (MAR) and the General circulation model (IPSL_CM4_D) for the same year averaged over the different regions of interest (see Figure 2).*

3.3. - The future climate experiments

The boundary conditions for the BIOLIM experiments are obtained from the different GCM simulations, which results are described in BIOCLIM Report D4/5 [Ref.1]. A summary of these simulations is given in Tableau 1.

We want to stress the important point already highlighted in the previous section. The IPSL_CM4_D results presented in BIOCLIM Report D4/5 [Ref.1] are mean values over the last 30 years of the simulation. However the MAR simulations were forced by one single year, arbitrarily chosen. Indeed it was too time consuming to run the MAR model for multiple years and there is not a single year that directly corresponds to the average over 30 years. This is the reason why it was decided to use a particular year, which may be significantly different from the 30-yr average. Therefore the figures are showing both the 30-yr average from the IPSL_CM4_D simulation and the particular year, interpolated on the MAR grid and including the altitude

effect. In addition to the MAR fields a composite variable is also displayed. The purpose of this variable is to extract from the MAR field the part of the signal that is produced by the IPSL_CM4_D model. This component is then added to the 30-yr average field from the IPSL_CM4_D model. This can be written as:

$$IPSL\_CM4\_D + (MAR - IPSL\_CM4\_D)$$

where *IPSL_CM4_D* represents the 30-yr average field, IPSL_CM4_D is the same field for the chosen year and MAR is the simulated field in the MAR model for the same year.

The following sections present the results for the BIOCLIM experiments performed with the MAR model. Namely, maps of 2-m high air temperature and precipitation are displayed for winter (DJF) and summer (JJA). They are showing anomalies with respect to a reference simulation (either the baseline or another BIOCLIM experiment).

3.4. - Simulation A

This simulation corresponds to a three times increase of atmospheric CO_2 concentration (1100 ppmv) under the present-day astronomical forcing and with the present-day extension of the continental ice sheets. The IPSL_CM4_D simulation already highlights the global warming related to the CO_2 increase. In DJF, the largest temperature increase is located in Northern Europe in the average mean, although it is more northeastward in the single year. The regional model simulates very large anomalies over most of Europe. These anomalies are slightly smaller over Spain, south of France and the Mediterranean basin in general. However the choice of a single year for both the baseline and the simulation A partly explains these anomalies (Figure 5a). It reaches up to 5°C in Spain, up to 6°C in England, north of France, Germany, and the Czech Republic. In JJA the largest increases simulated by IPSL_CM4_D are over western continental Europe, north of Italy, south of France and Northeast of Spain, with temperature increases of more than 5°C (Figure 5b). However, the temperature increase for the single year is much larger. Temperature increases by more than 6°C for most of Europe south of 50°N. Therefore the regional model simulates the strongest increase over Spain (more than 6°C). All the Mediterranean countries experience large temperature increases (up to 5°C in Italy and up to 6°C in Greece). There is a large SW-NE gradient in the temperature change over France (from 6°C to 4°C). The temperature increase is lower than 3.5°C in North Germany and lower than 3°C in central Czech Republic. It is between 3 and 4°C in Central England. However most of this warming is due to the choice of a particular year. When this factor is taken away, the temperature increase is much smaller. It hardly reaches 6°C in the SW of the Iberian Peninsula; it is about 3°C over Central England and about 2°C in NE France, N Germany and Czech Republic. Values for the study areas are given in Tableau 3.

The large difference between the precipitation patterns for the 30-yr average and the single year, both for DJF and JJA (Figure 5c-d), clearly illustrates the large interannual variability and makes it difficult to draw any definite conclusion about the precipitation pattern under high CO_2 atmospheric concentration. Moreover the regional model is simulating a strong spatial variability. Values for the study areas are given in Tableau 3.

Simulation A	MAR				IPSL_CM4_D			
	T. Surf.		Prec.		T. Surf.		Prec.	
	DJF	JJA	DJF	JJA	DJF	JJA	DJF	JJA
France	3.9	25.3	3.64	0.54	5.6	29.4	4.48	0.59
Spain	8.5	28.4	4.58	0.06	11.7	26.3	4.16	0.01
C.England	3.5	21.4	3.71	0.57	7.2	21.1	3.10	0.92
Czech R.	-3.4	23.4	1.24	0.77	2.3	25.5	2.01	2.61
Germany	-0.8	26.0	2.04	0.64	4.6	27.3	2.69	1.85

Table 3: *Simulation A. Surface temperature (°C) and precipitation (mm.day^{1}) in DJF and JJA as simulated by the regional climate model (MAR) and the General Circulation Model (IPSL_CM4_D) for the same year averaged over the different regions of interest (see Figure 2).*

3.5. - Simulation E

In this experiment the orbital parameters are those expected at 67 kyr AP. In the Northern Hemisphere this change leads to insolation larger than present day during Summer and lower than present day in Winter. Atmospheric CO_2 concentration is set at the present-day value as well as the ice sheets. Therefore the anomalies shown in Figure 6 only reflect the effect of the solar forcing change.

In DJF, Europe is only experiencing small temperature changes (Figure 6a). The largest decrease occurs in Spain (between -0.5° and -1°C). However the single year is exhibiting larger temperature decreases, i.e. at least -1°C over most of the continental Europe to -3°C over central Europe. The regional model amplifies the cooling simulated by IPSL_CM4_D. The temperature decrease simulated over Poland and central Europe is larger than 6°C. It is only up to –2°C over Spain. England hardly undergoes any cooling. The temperature even increases over Ireland, Scotland and Wales. In JJA, IPSL_CM4_D is showing a significant warming of up to 4°C in Eastern Europe and in the Alpine Countries (Figure 6b). However the warming is much larger (larger than 6°C) in the single year simulation. Moreover it is located further northeastward than in the 30-year average. The regional model simulates smaller temperature increases. In Western Europe, only Spain exhibits a temperature change larger than 6°C. Over most of Western Europe change is smaller than 4°C. Moreover, if temperature change is adjusted then temperature over Continental Europe, except Spain, is decreasing. Values for the study areas are given in Tableau 4.

In DJF, IPSL_CM4_D is showing a slight increase in precipitation over Spain and the Mediterranean (Figure 6c). The same pattern is valid for the single year although it is much more enhanced. Although more patchy, the pattern of precipitation change simulated by the regional model is similar to the IPSL_CM4_D one. Nevertheless, the Mediterranean coast of Spain is experiencing some precipitation decrease and the decrease in precipitation over Germany is larger in the regional model than in IPSL_CM4_D. The adjusted field is showing a general reduction of precipitation compared to the unadjusted one. In particular, precipitation in central and south of Spain is smaller than in the baseline. In JJA, IPSL_CM4_D is showing a decrease in precipitation over France, north of Spain and central Europe (Figure 6d). As for DJF, this pattern is enhanced in the single year. The regional model is also showing a reduction of the precipitation over north of Spain, south and east of France, north of Italy and the eastern coast of the Adriatic and Ionian seas. However, adjusted precipitation is showing a decrease over Spain. Moreover the decrease in Northern Europe is strongly enhanced and it extends much more southward, including north of France and Germany. Values for the study areas are given in Tableau 4.

Simulation E	MAR				IPSL_CM4_D			
	T. Surf.		Prec.		T. Surf.		Prec.	
	DJF	JJA	DJF	JJA	DJF	JJA	DJF	JJA
France	-7.0	23.2	3.43	0.58	0.6	28.9	3.80	1.09
Spain	2.1	27.2	4.90	0.10	8.6	24.7	5.12	0.08
C.England	-3.8	20.6	4.02	0.78	3.8	22.3	3.22	0.27
Czech R.	-16.7	23.5	1.32	1.22	-4.2	26.3	1.72	2.40
Germany	-15.1	26.3	1.82	1.84	-2.1	28.4	2.52	1.75

Table 4: *Simulation E. Surface temperature (°C) and precipitation (mm.day^{-1}) in DJF and JJA as simulated by the regional climate model (MAR) and the General Circulation Model (IPSL_CM4_D) for the same year averaged over the different regions of interest (see Figure 2).*

3.6. - Simulation D

The orbital parameters for 67 kyr AP are used to compute the solar forcing of this simulation. Moreover it is assumed that there is no Northern Hemisphere ice sheet. Similarly to what was done in BIOCLIM Report D4/5 [Ref.1], we will first present the anomalies as differences from Simulation E. This should highlight the role of the present-day Greenland ice sheet on the climate at 67kyr AP. In both Winter and Summer the IPSL_CM4_D experiment is showing a cooling in the northern part of the domain (north of 50N, including Great Britain) and a warming in the southern part of the domain (Figure 7a-b). The feature is valid for both the 30-yr average and the single year used to force the regional model. However the cooling in the north and along the Atlantic coast is enhanced in the single year. The regional model is exhibiting a DJF cooling of -0.5°C over Western Europe (from Spain to Poland) and a warming over the Eastern Mediterranean and central Europe of up to 6°C in the north of Yugoslavia. In Summer, the cooling is affecting most of Europe. It is centred over Belgium with a value of -4°C. However, when adjusted, Southwestern Europe (mostly Spain and France) experiences a warming of up to 3°C and the Northeastern Europe is cooling, the strongest cooling being –3°C over the Baltic countries.

Winter conditions simulated by IPSL_CM4_D are usually wetter in Simulation D than in Simulation E in the South (except off the Mediterranean coast of Spain) and drier in the North (Figure 7c). This pattern is strongly enhanced in the single year. According to the regional model, Spain is experiencing much wetter conditions. It is also the case for the Southern Alps. However precipitation decreases over most of Great Britain, central France. The Summer precipitation changes are very small in the 30-yr average (Figure 7d), with an increase of 0.6mm.day^{-1} over Great Britain. However, the selected single year is particularly wet compared to E over an area extending between 45 and 55°N, from Ireland to Poland. In the regional model, the changes in precipitation are not strongly significant in Spain, France, Great Britain and central Germany but there is a strong decrease in precipitation over north of Germany, which extends to north of France for the adjusted field.

The comparison between IPSL_CM4_D simulation D and the IPSL_CM4_D control simulation shows a DJF cooling in the North (Figure 8a), probably related to the removal of the Greenland ice sheet, and a JJA warming (Figure 8b), probably due to the orbital forcing. The regional model simulates a cooling along the Atlantic coast up to Russia. This feature is similar to the D – E feature, suggesting that it is related to the removal of the Greenland ice sheet. In Summer there is a strong warming over the whole domain except over north of Poland. The adjusted field also displays a slight cooling over north of England. These Summer features could be related to the change in the orbital forcing (see simulation E above). Values for the study areas are given in Tableau 5.

The precipitation changes in IPSL_CM4_D relative to the control are mostly related to the orbital change in DJF (Figure 8c) while the JJA (Figure 8d) increase in the north of the domain can be attributed to the removal of the Greenland ice sheet. In the MAR model DJF is undergoing stronger precipitation in D than now over south of Europe (Spain, Italy, former Yugoslavia, Greece) and up to Ukraine. This feature is similar but stronger than in the comparison D–E. Moreover, the adjusted precipitation field is showing a wetter pattern over almost all the European continent. The maxima of precipitation increase in DJF occur over Spain and Austria. In JJA the pattern is less clear, with large regional variability. Nevertheless, Massif Central, Vosges and Jura, Alps region, Black Forest are wetter than in the baseline simulation. Values for the study areas are given in Tableau 5.

Simulation D	MAR				IPSL_CM4_D			
	T. Surf.		Prec.		T. Surf.		Prec.	
	DJF	JJA	DJF	JJA	DJF	JJA	DJF	JJA
France	-7.4	23.6	2.91	0.95	-0.3	24.0	2.44	2.66
Spain	0.5	27.4	6.38	0.14	7.6	242	4.42	0.14
C.England	-3.7	19.3	2.89	0.99	2.2	19.0	2.13	1.33
Czech R.	-14.9	21.8	2.02	1.43	-4.0	21.7	1.69	3.62
Germany	-15.4	23.3	2.01	0.70	-2.9	24.2	2.10	2.86

Table 5: *Simulation D. Surface temperature (°C) and precipitation (mm.day^{-1}) in DJF and JJA as simulated by the regional climate model (MAR) and the General Circulation Model (IPSL_CM4_D) for the same year averaged over the different regions of interest (see Figure 2).*

3.7. - Simulation C

In this experiment, in addition to a change of the insolation forcing (67 kyr AP), CO_2 forcing is increased up to 550 ppmv. Moreover it is assumed that Greenland has completely melted. Therefore this simulation will first be compared to simulation D, in order to identify the impact of a CO_2 increase on a climate different from the present-day one. The global pattern of climate change, as shown in the 30-yr average IPSL_CM4_D simulation, is very similar to the present-day pattern of change under a tripling of CO_2 concentration, but with smaller amplitude. However the single year boundary conditions are rather different. In DJF, surface temperature (Figure 9a) in C simulated by the regional model is much larger (more than 9°C over Slovenia, and more than 7°C over central Germany) than in D over most of the continental western and central Europe but the adjusted temperature shows a smaller change, i.e. temperature increase hardly reaches 6°C north and east of the Alps. The summer (JJA) warming in C compared to D (Figure 9b) is smaller than the winter one. Moreover it is localised more southward. In IPSL_CM4_D the warming is centred over Greece, both for the 30-year average and the single year. However the single year warming is enhanced compared to the average value. Similarly the MAR warming concentrates on the Mediterranean with the largest values over southeastern Spain, South of Italy and of Greece. The adjusted values show a general similar pattern, although with a smaller amplitude. Moreover there is also a warming (compared to D) North of England and over Scotland. Values for the study areas are given in Tableau 6.

The MAR simulated pattern of precipitation in DJF exhibits a strong North-South gradient (Figure 9d). Precipitation decreases south of 45N and increases north of that latitude. However the adjusted pattern is patchier. There is a large precipitation increase over the NE of Spain and the SW of France, and over Italy. The precipitation change is very small over Germany and the Czech Republic. Precipitation increases over Scotland. IPSL_CM4_D shows almost no change in the precipitation pattern in summer (Figure 9d). However the single year is showing a strong 'seesaw', with reduced precipitation in the Northeast of the domain (Baltic countries, Belarus) and larger precipitation over North of France, Belgium and part of central-west Germany, and, although less intense, over Hungary, Italy, former Yugoslavia, Bulgaria. The MAR model does not simulate a clear general pattern, although there is a rather general increase in precipitation, except over Austria and the Czech Republic. Moreover this drying pattern extends further over most of western and Central Europe for the adjusted precipitation field. Values for the study areas are given in Tableau 6.

Although the comparison between C and the control, on the one hand, and D and the control, on the other hand, show similar features for the DJF 30-yr average, the selected single years (compared to the control) are significantly different. Therefore the simulated MAR climate is also different. There is a Winter warming over most of Europe (Figure 10a), except for the countries along the Baltic Sea. The warming is also less pronounced over Spain, SW of France and the Alps. In summer, D minus control (Figure 8b) and C minus control (Figure 10b) are showing a very similar pattern of temperature change, both for the 30-yr average and the single year, although the temperature increase in C is somewhat larger than in D, compared to the baseline. Consequently, temperature increase affects most of Europe. It is larger in the South and smaller in the North.

The DJF precipitation change is drastically different for C–control compared to D–control (Figure 10c and Figure 8c). In fact the selected IPSL_CM4_D years are very different from each other, and also from the 30-yr average. Compared to the control, the C simulation in IPSL_CM4_D shows a strong NW-SE gradient of change. Precipitation increases for the countries along the Atlantic Ocean and it decreases over the Mediterranean Sea. According to MAR, the precipitation increase is located in Portugal, Brittany, Great Britain, Belgium and Northern Germany, as well as over the Alps. Eastern Spain and south of France, as well as Southern Italy, are drier. The adjusted precipitation field is showing a drier continental Europe, except for Southern Spain, the Alps and the Dinaric Alps. In summer, IPSL_CM4_D simulates a reduction of precipitation over most of continental Europe (Figure 10d). It is even stronger over the selected year. The regional model confirms these drier conditions, except for Central Europe. Indeed, Austria, Czech Republic, Slovakia, Hungary undergo an increase in precipitation of up to 0.6mm.day^{-1}.

Simulation C	MAR				IPSL_CM4_D			
	T. Surf.		Prec.		T. Surf.		Prec.	
	DJF	JJA	DJF	JJA	DJF	JJA	DJF	JJA
France	3.3	24.0	4.13	0.56	5.1	27.1	4.73	1.22
Spain	6.9	28.8	4.56	0.03	10.5	25.6	3.37	0.02
C.England	1.2	19.3	4.90	0.83	6.0	19.4	4.34	0.83
Czech R.	-5.2	22.4	2.24	1.84	1.4	23.5	2.62	2.96
Germany	-5.8	24.1	3.39	1.05	2.5	25.2	4.21	2.07

Table 6: *Simulation C. Surface temperature (°C) and precipitation (mm.day^{-1}) in DJF and JJA as simulated by the regional climate model (MAR) and the General Circulation Model (IPSL_CM4_D) for the same year averaged over the different regions of interest (see Figure 2).*

3.8. - Simulation B

This simulation is performed under present-day insolation forcing. A high CO_2 atmospheric concentration (550 ppmv) is assumed as well as the complete melting of the Greenland ice sheet. This simulation will be compared to simulation C in order to identify the impact of the insolation forcing on climate. This comparison is similar to the comparison (E – baseline) although this last one takes place with a present-day Greenland ice sheet (Figure 11 is showing C–B anomalies). In DJF, Europe is only experiencing small temperature change (Figure 11a). The large increase is seen over the northeastern part of the domain. It is most probably related to the indirect effect of insolation change, such as the snow/ice-albedo-temperature feedback. However the selected IPSL_CM4_D years for the MAR simulation are very much different (from each other and from the average in the case of simulation B). In the C simulation, this single year experiences a very strong Winter warming over central Europe compared to B. All the MAR domain, except for Scotland is warmer in this IPSL_CM4_D simulation. Although the MAR model is also showing a large increase over the whole European continent the amplitude of this change is strongly enhanced, with, for example, a warming of more than 16°C over Hungary. The adjusted change is still showing large temperature increases over the whole continent. In Summer (Figure 10b), both the 30-yr average and the single year are showing a warming. There is an increasing West-East gradient in the 30-yr average, while this gradient is more NW-SE in the single year. In the regional model the warming is larger in the southern part of the continent (mostly Spain, Italy and Greece). In the North (Great Britain, Denmark, North Germany, Baltic countries) there is only a small warming, if any. However the warming affects all the continent if the use of a single IPSL_CM4_D-yr is taken into account. Values for the study areas are given in Tableau 7.

The MAR simulated pattern of precipitation in DJF (Figure 11c) exhibits a strong North-South gradient, as for C–B. Precipitation increases north of 45N and decreases south of that latitude (except for the western part of the Iberian Peninsula). However, the adjusted pattern is patchier. Most of Spain experiences wetter conditions in C than in B, except for the Northeast. France is drier but the alpine region receives more precipitation. Great Britain, Belgium, Germany and the Czech Republic are also wetter. Although not uniform, there is a general pattern of decreasing precipitation over Europe in Summer (Figure 11d). There are some exceptions for Central England and Scotland, Northeast of Spain and Hungary. However the adjusted precipitation field is displaying an enhanced drying over North of Spain, South of France; Italy, Austria and Croatia and Slovenia, while precipitation increases over North of France, Belgium, The Netherlands, Denmark, as well as Ukraine. Values for the study areas are given in Tableau 7.

Simulation B will now be compared to the baseline simulation (Figure 12). The differences in the response are now related either to the increase in CO_2 concentration or to the melting of the Greenland ice sheet. In the 30-yr average IPSL_CM4_D, the temperatures over Southern Europe are generally warmer than at present (Figure 12a), but they are cooler over Northern Europe. However the pattern of temperature change is very much different over the single selected year for DJF. For that specific year the northern cooling extends to the South over the whole domain. It is more than -6°C over Ukraine and still larger then -0.5°C over Spain. Only Scotland and Ireland are experiencing a warming. Consequently the temperature simulated by MAR are much cooler in B than in the baseline. The cooling is reduced along the Atlantic coast, Spain, the Alps and Southern Italy. Moreover, temperature over Great Britain is warmer in B than at present when adjusted, cooling over Europe is still the dominating feature although it is significantly reduced. The pattern of temperature change for JJA (Figure 12b) in the single IPSL_CM4_D year is showing a warming over all the European continent, except for Belarus and Russia. The maximum temperature change is centred over the Pyrenees (+4.5°C). MAR is simulating a maximum Summer warming compared to present in Spain (+3.5°C). The warming is still large over the Mediterranean region (+2.5°C over Italy and Greece). The lowest warming is simulated coming from Russia through Belarus, Poland and Northern Germany.

However the adjusted Summer temperature are cooler over almost all Europe, except Spain, Italy and Greece, and the Baltic countries.

In terms of precipitation, IPSL_CM4_D shows a decrease over Northern France and Southern Spain in DJF (Figure 12c). In JJA, there are decreases over Southern Europe, and increases over Great Britain (Figure 12d). Both in DJF and JJA, these precipitation features are strongly enhanced in the single IPSL_CM4_D year. In Winter the IPSL_CM4_D pattern is broadly reproduced by MAR, except for the Mediterranean coast of Spain and France, which experience wetter conditions. However the corrections of the precipitation field cancel out, more or less, the large decrease of precipitation. Some drier areas remain, mostly over Germany. In Summer time, there is no coherent pattern of precipitation change over large areas but rather a large regional variability.

Simulation B	MAR				IPSL_CM4_D			
	T. Surf.		Prec.		T. Surf.		Prec.	
	DJF	JJA	DJF	JJA	DJF	JJA	DJF	JJA
France	-10.3	22.5	2.37	1.01	-0.4	23.6	2.56	2.54
Spain	-0.1	24.8	3.24	0.06	8.5	23.8	2.44	0.20
C.England	-2.2	18.8	2.11	0.84	4.0	18.3	1.88	1.34
Czech R.	-18.1	20.8	1.74	1.39	-5.9	20.2	1.95	3.76
Germany	-17.3	23.2	1.82	1.46	-2.8	22.2	2.32	3.48

Table 7: *Simulation B. Surface temperature (°C) and precipitation (mm.day^{1}) in DJF and JJA as simulated by the regional climate model (MAR) and the General Circulation Model (IPSL_CM4_D) for the same year averaged over the different regions of interest (see Figure 2).*

3.9. - Simulation F

In simulation F there are moderately large ice sheets over the Northern Hemisphere. The atmospheric CO_2 concentration is set to an interglacial level (280 ppmv) and the orbital parameters are computed for 178 kyr AP. For the Northern Hemisphere, it means larger insolation during Spring and early Summer and lower values during late Summer and Autumn. In DJF, IPSL_CM4_D is therefore showing a small cooling in Northern Europe but most of Continental Europe is experiencing only small temperature changes (Figure 13a). However the single year used as a boundary condition for MAR shows a larger cooling, especially over Western Europe. The regional climate model simulates cooling over most of Europe. The largest temperature decrease is experienced over France (-6°C). This cooling extends to Poland (-4°C) and north of Spain (-3.5°C). This cooling is slightly reduced in the adjusted field. There is even a slight warming south of Spain and south of Italy (0.5°C). In Summer the presence of the ice sheets in the North induces large cooling over Northern Europe according to IPSL_CM4_D (Figure 13b). However warmer conditions prevail over North Africa, related to the insolation change. These warm conditions extend up to 50°N in the single year simulation. The regional model identifies clearly a warming over Spain. The cooling over the northern part of the domain extends more southward in the adjusted field. The largest cooling (-4.5°C) occurs over Germany. Values for the study areas are given in Tableau 8.

In DJF the precipitation changes are dominated by a localised increase over the Atlantic, off the Portugal coast (Figure 13a). This increase simulated by IPSL_CM4_D is even stronger in the selected year.

Moreover it extends over most of the Mediterranean basin. On the other hand there is also a sharp reduction of precipitation over the North Sea, with some implication for all the neighbouring countries. The MAR domain is divided into two parts with respect to DJF precipitation. The South (mostly Mediterranean countries) is experiencing wetter conditions and the North, drier conditions. The gradient is smoother for the adjusted fields. The pattern is rather different for Summer time (Figure 13d). There is a large decrease of precipitation over Southern Europe (centred over Switzerland and Austria). Moreover this decrease of precipitation is much larger for the single year and it extends over most of the western countries, except Great Britain, where precipitation increases over most of the country. The regional model simulates a less extended area of precipitation decrease, especially for the adjusted field. Indeed in that case, most of Europe experiences wetter conditions. Only the Cantabrian mountains, the Alps and the Dinaric Alps are drier. Values for the study areas are given in Tableau 8.

Simulation F	MAR				IPSL_CM4_D			
	T. Surf.		Prec.		T. Surf.		Prec.	
	DJF	JJA	DJF	JJA	DJF	JJA	DJF	JJA
France	-9.5	20.2	2.61	1.06	-0.6	22.5	2.92	0.75
Spain	1.7	25.6	5.96	0.03	7.7	23.1	4.10	0.08
C.England	-5.4	16.0	2.64	0.99	2.1	15.3	2.16	1.20
Czech R.	-15.0	18.7	1.34	1.62	-3.3	20.2	1.86	2.39
Germany	-13.3	19.6	1.86	1.38	-3.0	21.3	2.14	1.96

Table 8: *Simulation F. Surface temperature (°C) and precipitation (mm.day^{-1}) in DJF and JJA as simulated by the regional climate model (MAR) and the General Circulation Model (IPSL_CM4_D) for the same year averaged over the different regions of interest (see Figure 2).*

4. Time series over the European Study Areas

Timeseries of temperature, precipitation, snow, wind and radiation averaged over the different regions of interest (see Figure 2) are presented in this section.

4.1. - 2m air temperature

The 2m air temperature is displayed in Figure 14 for the different European regions. Simulation A is warmer than the control almost all the year round for the different sites. The difference between this simulation and the control becomes small (or temperature can even become lower than the control) in December. In March, this difference also becomes small for the Central England, German and Czech study areas, but this is probably related to internal variability rather than a robust feature.

According to simulation B, Germany and the Czech Republic are colder than the baseline at the end of Autumn, in winter and early Spring. The summer warming is very small. Although less clear the pattern seems to be similar for Spain and France. In Central England, the deviation from the baseline is smaller than for the other regions and there is no clear trend. Unfortunately this experiment may be strongly biased by the use of single years for the MAR simulations. This could explain the unexpected cooling although atmospheric CO_2 concentration increases and the Greenland ice sheet is melted.

Simulation C is warmer than the baseline all the year and for all the regions, except in March in Central England, France, Germany and the Czech Republic. This last feature is probably not robust and could be related to interannual variability. In the different regions, simulation C is warmer than simulation B most of the year (the major exception is March), although insolation is larger in C than B only during summer time. This points out a feedback process (such as the albedo-temperature feedback) to explain the difference in temperature.

Simulation D is showing cooler Spring and Autumn seasons than the control simulation, except for Spain, which is warmer than the control all the year. The Summer season is warmer. The Summer warming is the largest over the Spanish region. There is no general trend for Winter. Moreover, it is also suspected that there is a large interannual variability. Indeed, let us remind that all the simulations are performed over 15 months and plotted from December year 1 (month 0 on the figures) to December year 2 (month 12). The comparison between the values for the two December months of the simulation shows a large difference. The temperature changes in Spring, Summer and Autumn can largely be related to the changes in insolation between the present and 67 kyr AP. Although the CO_2 concentration is larger in C than in D, the surface temperature in C is lower than in Simulation D for some months. However this behaviour could be related to the choice of the boundary conditions.

Simulation E is showing a stronger seasonal cycle than the control. It is also enhanced with respect to the D simulation. However Summer temperatures (June, July) in France and Spain are not larger than in the D simulation, as is the case for the other regions.

In simulation F, temperature is colder than the control throughout the year (except in June) in Central England, France, Germany and the Czech Republic. Again the comparison between the two December months clearly suggests a strong interannual variability. The second December month is 5°C warmer than the first one over Central England. This simulation is also the coldest one for Central England. However, from February to May the temperatures over Spain in F and the control are very similar. It is even warmer in F than in the control from June to August.

4.2. - Total precipitation

The total precipitation is displayed in Figure 15 for the different European regions. For all the experiments, the seasonal cycle of precipitation is showing the largest amplitude in Spain (8 mm.day^{-1} in the D simulation) amongst the five regions. It is much smaller in Germany and Czech Republic (of the order of 4 mm.day^{-1}). It has an intermediate value in Central England and France (5 mm.day^{-1}). Moreover, the seasonal cycle in these two areas is still marked by a Summer minimum of precipitation and possibly a secondary minimum in Winter. On the contrary the seasonal cycle in Germany and Czech Republic is dominated by the month to month variability. It must also be mentioned that present-day simulated precipitation for France is exhibiting a very large value for August, which is probably a feature of the selected year. This will prevent any comparison with the present for Summer time for the French area. Most of the experiments are showing an extended dry summer season (starting earlier, ending later).

The increase in atmospheric CO_2 concentration, as prescribed in simulation A, results in a decrease in precipitation in Spring and Autumn season in Spain and a slight increase in Winter time. There is almost no precipitation during Summer. In the other regions the variability is very large from one month to the next and also probably the interannual variability. Therefore it is difficult to extract any robust trend. Nevertheless it seems that, like in Spain, Spring and Autumn precipitation increases in the A simulation compared to the present although there is no precipitation in September. In fact, September seems to be a very dry month in simulation A. This is most probably a feature of the IPSL_CM4_D year used as boundary condition rather than the feature of the mean climate. July and August are also drier than the present in Germany and Czech Republic.

Spain is undergoing a decrease of precipitation most of the year in simulation B (except in March and the final December). Annual mean precipitation increases in Germany and the Czech Republic although some months can be drier (e.g. December to April in Germany). In central England and France the variability is too large to allow the determination of any clear trend.

Simulation C is drier most of the year in Spain (except in December). It is not the case in the other regions. They are undergoing large month to month variability with a very slight tendency to wetter conditions in annual mean precipitation.

From February to May and from August to October, simulation D is wetter than the present over Central England. Spring is also wetter than present in France. Late Autumn, Winter and Early Spring are much rainier than the present in Spain. Like for the present there is almost no rain from June to September in Spain. On the contrary most of the year is drier than present in Germany. However the precipitation changes are very small (less than 1 mm.day^{-1}).

Simulation E is similar to simulation D, except that Greenland is completely melted in D. A general feature for Central England and France is that Winter precipitation is larger in E than in D, and it is the reverse for the rest of the year. In Spain, on the contrary, precipitation is smaller in E than in D from October to March; it is larger in April-May; and there is almost no precipitation in Summer. No clear trend can be detected for Germany and Czech Republic.

In simulation F, which corresponds to insolation forcing at 78 kyr AP, precipitation is larger than at present in Spring over Central England and France. This is also the case in Central England in Autumn. But it is smaller than at present in Winter. From September to April precipitation is much larger than present over the Spanish region. In Germany and the Czech Republic precipitation has a tendency to be slightly larger in F than at present all the year round except in Winter.

4.3. - Snow fall

Snowfall is displayed in Figure 16 for the different European regions. Simulation A shows a sharp decrease in Winter snow fall over the different regions. The decrease in simulation C is as sharp as in simulation A in Spain. However there is a large increase in snowfall in Central England and Germany in late winter and early Spring. There is no clear trend in snowfall for simulation B neither amongst the different regions, nor over the year. At the end of the melting season and at the time of the very beginning of the accumulation season, snow fall is reduced in C compared to B. This explains the warmer temperatures in C than in B during these times of the year. Simulation D is displaying a significant late Spring increase in snowfall over Central England and France, while the Autumn and Winter snow precipitation is decreasing. Germany and Czech Republic also see an increase in snowfall in Spring but snowfall increases in Autumn. Simulation E, compared to the present, is showing the largest increase in snowfall over France and Central England. It is especially large over Winter and Spring. Spain and Germany also experience an early Spring increase in snowfall. In simulation F, the different regions, except the Czech Republic, experience an increase of snow fall in Spring as well as in Autumn, compared with the present. Moreover snowfall starts one to two months earlier in F than at present. In the Czech Republic, snow precipitation increases only in late Spring. There is also a sharp increase in September, which could be related to interannual variability.

4.4. - Wind speed

Wind speed is displayed in Figure 17 for the different European regions. An overview of the figure shows that the variability is larger in Central England and France than in Germany and the Czech Republic. Moreover there seems to be a slight seasonal cycle in wind speed in Spain, with a minimum in summer time and large values in December.

In Central England wind speed is not very much affected by the increase in atmospheric CO_2 concentration in simulation A. However in France, for the same simulation, wind speed increases in Spring and decrease in Autumn, compared to the present-day values (changes are of the order of 1m/s). In Spain, there is a small general decrease in wind speed in simulation A, except in January and February. No general feature can be identified for Germany and Czech Republic in the simulation A.

In simulation B, wind speed has a tendency to decrease in Winter-Spring time and to increase very slightly in Summer-Autumn in Central England and Germany. In the Czech Republic the wind speed is larger in B than in the baseline most of the year (except March and November). The sign of the deviation from the baseline in France changes from one month to the other.
Spring, Summer and early Autumn see a reduction of the wind speed in France in simulation C. The increase in wind speed in early spring seems to be a general feature of the different regions.

In simulation D wind speed increases from late Summer to end of February in Central England, when compared to the present-day. In France the increase in wind speed occurs mostly in Spring (from January to May), although there is also a small increase in Autumn. This picture is enhanced over Spain. The largest increase in wind speed occurs in March (more than 2.5m/s). Late Autumn and Winter are also undergoing higher wind speeds (+2m/s). On the contrary, Germany and the Czech Republic are less windy in early Spring and late Autumn.

In simulation E wind is less strong in Spring over Central England and France than in the baseline and in simulation D. This could probably be related to a change in the wind pattern related to the melting of the Greenland ice sheet. It is also less windy in E than in D in Autumn over Central England. In Spain wind is less strong for simulation E than D almost all the year round,

except in May. However it is larger in E than at present in late Winter and Spring. In Germany and the Czech Republic, wind strongly decreases in E with respect to D and the present from February to June. However it is higher than the baseline in Summer and Autumn in the Czech Republic. Simulation F is showing large wind speed increases in Autumn for the different regions, e.g. +2m/s in September over Central England, +1.7m/s in October in France, +2m/s in November in Spain, +2m/s in September in Germany, +0.8m/s in September in the Czech Republic. In Central England, France, Germany and the Czech Republic, some Spring months undergo wind speed reduction. However Spring in Spain is also windier in F than at present.

4.5. - Soil downward short wave and longwave radiation

The soil downward short wave and long wave radiation are displayed in Figure 19 and Figure 20 respectively for the different European regions. The amount of solar radiation absorbed at the ground level is very much dependent on the amount of solar energy available at the top of the atmosphere. Therefore experiments A and B are showing a pattern similar to the control. Experiments D, E and F are showing an increase in SW during the Spring and Summer months and a decrease in SW during Autumn. The downward shortwave radiation at the surface is very closely related to the surface temperature. In Germany and the Czech Republic there is a large increase in shortwave radiation in July in experiment E.

5. Conclusions

While the large-scale patterns of surface climate change in the nested (MAR) and driving (IPSL_CM4_D) models are similar, the regional details of the simulated changes can be enhanced in MAR. For example, in experiment E, the change in orbital forcing induces a large decrease of DJF precipitation over Spain at the large scale, whereas there is strong North/South gradient at the regional scale (Figure 6c), with a large rainfall increase in northern Spain, a much smaller one in the South, and even some decrease along the Mediterranean coast. In summer France experiences a large warming (more than 5°C over most of the country) at the global scale (Figure 6b). However the warming is not so large anymore at the regional scale and there are many geographical differences (Figure 6b). The largest warming occurs in the West. The Alps and the Massif Central are warming less. These differences are more clearly seen in mountainous areas. It is also the case, for example, for the DJF temperature increase in Simulation C compared to the baseline (Figure 10). It is more reduced over the Alps than in the surroundings areas. The regional response of the Mediterranean islands are also enhanced in MAR compared to IPSL_CM4_D. For example, in experiment A and D, the warming is larger over Corse, Sardinia and Sicily (land) than over the surrounding Mediterranean Sea (sea).

According to IPCC [Ref.17] *the high resolution representation of mountainous areas in region al climate models has made it possible to show that the simulated surface air temperature change signal due to 2 x CO_2 concentration could have a marked elevation dependency, resulting in more pronounced warming at high elevation than low elevation* [Ref.18 ; Ref.19]. The MAR response is slightly more qualified or, rather, some seasonal dependencies are suggested. In experiment A, the three-fold increase in CO_2 concentration, the winter warming is strongly reduced over the Alps, as well as over the Apennines and the Balkans compared to the plains (Figure 5a). However the Apennines and the Balkans experience larger warming in Summer compared to less elevated regions (Figure 5b). The increase of CO_2 concentration at 67 kyr AP (from 345 to 550 ppmv) (experiment C compared to D, Figure 9a), induces a similar response in winter over the elevated regions. In summer (Figure 9b), the warming over the Alps, southern Italy and Greece, Albania and Macedonia is much large than over most of Europe.

Over the different regions of interest, MAR is showing colder temperatures in winter than IPSL_CM4_D for the same year, especially over the north-eastern part of the domain, such as in Poland and Belarus (see for example experiments E, D and B, Figure 6b, Figure 8a, Figure 12a). This cooling of MAR compared to IPSL_CM4_D appears also in summer for experiment F (Figure 13b). More generally speaking, MAR is enhancing the temperature response of IPSL_CM4_D during winter. This response of the MAR model can be related to changes in regional feedbacks, such as better taking into account the snow cover and related feedbacks. However this difference could also be an artefact of the computation of the temperature. Indeed, none of the models is explicitly computing surface temperature. Rather temperature at the surface (as well as 2m-high temperature) is interpolated/ extrapolated from temperature at higher levels. This procedure can induce large differences, especially during winter, when the continents are covered by snow.

The warming due to an increase in the CO_2 concentration (from the present to A and from D to C) is larger in Summer than in Winter over all the study areas except Spain. Precipitation change is much more site dependent. For the present day solar forcing, an increase in CO_2 concentration leads to a decrease in summer precipitation at all sites but for the 67 kyr AP solar conditions, Czech Republic and Germany are experiencing an increase in summer precipitation.

During winter the largest temperature changes are related to changes in the orbital forcing (between 67 kyr AP and the present) in France, Spain, Germany and the Czech Republic and in the CO_2 concentration in Central England. However the behaviour is slightly different in winter. The changes in the CO_2 concentration have the largest impact over France, Spain and Central England while the impact of the changes in orbital parameters (between 67 kyr AP and present) is the largest in the Czech Republic and Germany.

6. References

Ref. 1: BIOCLIM Report D4/5 (2003). Global climatic characteristics, including vegetation and seasonal cycles over Europe, for snapshots over the next 200,000 years. Available on www.andra.fr/bioclim.

Ref. 2: BIOCLIM Report D3 (2001). Global climatic features over the next million years and recommendation for specific situations to be considered. Available on www.andra.fr/bioclim.

Ref. 3: Berger, A., 1978. Long-term variations of daily insolation and Quaternary climatic changes, J. Atmos. Sci., 35, 2362–2367.

Ref. 4: Fouquart, Y. and Bonnel, B. 1980. Computation of the solar heating of the Earth's atmosphere: A new parameterization. Beitr. Phys. Atmos. 53: 35-62.

Ref. 5: Morcrette, J. 1984. Sur la paramétrisation du rayonnement dans les modèles de la circulation générale atmosphérique. Thèse de Doctorat d'Etat. Univ. des Sci. et Tech. de Lille, Lille.

Ref. 6: Gallée, H. 1995. Simulation of the mesocyclonic activity in the Ross Sea, Antarctica. Mon. Wea. Rev. 123 2051-2069.

Ref. 7: Therry, G. and Lacarrère, P. 1982. Improving the eddy kinetic energy model for the planetary boundary-layer description. Bound. Layer Meteor. 25: 63-88.

Ref. 8: Brasseur, O. 1999. Mesoscale modeling of extreme meteorological events over Belgium. Dissertation doctorale. Fac. des Sci. Appl., Univ. catholique de Louvain, Louvain-la-neuve.

Ref. 9: De Ridder, K. and Schayes, G. 1997. The IAGL land surface model. J. Appl. Meteor. 37, 167-182.

Ref. 10: Marbaix, P., Gallée, H., Brasseur, O., van Ypersele, J.P., 2003. Lateral boundary conditions in regional climate models: A detailed study of the relaxation procedure. Mon. Wea. Rev., 131 (3), 461-479.

Ref. 11: Gallée, H. and Schayes, G. 1994. Development of a three-dimensional meso-gamma primitive equations model. Mon. Wea.Rev. 122: 671-685.

Ref. 12: Fichefet, T., Campin, J.-M., Deleersnijder, E., de Montety, A., Goosse, H., Poncin, C., Tartinville, B., Huybrechts, P., Janssens, I., van Ypersele, J.-P., Gallée, H., Brasseur, O., Lefebre, F., Marbaix, P., Tricot, C; Fontaine, F., Mormal, P., Vandiepenbeeck, M. 2001. Modelling the climate system and its evolution at the global and regional scales (CLIMOD). Final Report. In Global Change and Sustainable Development, Subprogramme 1 : To Reduce Uncertainty, Federal Office for Scientific, Technical and Cultural Affairs, Brussels, 120 pp.

Ref. 13: Marbaix, P., 2000. A regional atmospheric model over Europe: adaptation for climate studies and validation. PhD thesis. Université catholique de Louvain. Institut d'astronomie et de Géophysique Georges Lemaître. Louvain-la-Neuve, Belgium. 174pp.

Ref. 14: Lefebre, F, Gallée, H, Van Ypersele, JP, Huybrechts, P, 2002. Modelling of large-scale melt parameters with a regional climate model in south Greenland during the 1991 melt season. Annals of Glaciology, 35, 391-397.

Ref. 15: De Ridder, K, Gallée, H, 1998. Land surface-induced regional climate change in southern Israel. J. Appl. Meteor., 37(11), 1470-1485.

Ref. 16: Brasseur, O., 2001. Development and application of a physical approach to estimating wind gusts. Mon. Wea. Rev. 129 (1), 5-25.

Ref. 17: IPCC,2001: Climate Change 2001: The Scientific Basis. Contribution of Working Group 1 to the Third Assessment Report of Intergovernmental Pannel for Climate Change.[Houghton, J. T., Ding, Y., Griggs, D. J., Nogueur, M., van der Linden, P. J., Dai, X., Raskell, K., and Johnson, C. A] Cambridge University Press, Cambridge, United Kingdom and New York, USA, 881 pp.

Ref. 18: Giorgi, F., Hurrell, J.W., Marinucci, M.R., Beniston, M., 1997. Elevation signal in surface climate change: A model study. J. Climate, 10, 288-296.

Ref. 19: Giorgi, F., Hewitson, B., Christensen, J., Hulme, M., Von Storch, H., Whetton, P., Jones, R., Mearns, L., FU, C., 2001. Regional Climate Information - Evaluation and Projections. In Climate change 2001 : The Scientific Basis. Contribution of Working Group I to the Third Assessment Report of the Intergovernmental Panel on Climate Change [Houghton, J.T., Ding, Y., Griggs, D.J., Noguer, M., van der Linden, P.J., Dai, X., Maskell, K., and Johnson, C.A. (Eds)]. Cambridge University Press, Cambridge, United Kingdom and New York, NY, USA, 881pp.

Appendix A

Several variables have been archived on a monthly mean basis and are available to the BIOCLIM partners on www.andra.fr/bioclim :

MAR_X (X stands for the experiment name) files
Each archived file (ASCII format) corresponds to one simulated year. For each grid point a table gives the value of the given variable for the 13 months in the year (December to December). Only monthly mean values are provided for each simulated years.

The following variables are available
- Precipitation (total and snow)
- Surface (SBL) air humidity
- Cloud optical depth
- Soil downward shortwave radiation
- Soil downward longwave radiation
- Air (SBL) temperature
- 2m- air temperature
- Surface temperature
- Wind speed

Values are available for each grid point in each region of interest (Figure 2).

BIOCLIM_MAR_X_Region.res (Region stands for the name of the different study areas) **files**

Each archived file (ASCII format) corresponds to one simulated year. The table gives the value of the given variable (see above the list of variables) for the 13 months in the year (December to December) averaged over the study area (Figure 2). Only monthly mean values are provided for each simulated years.

Appendix B : List of figures

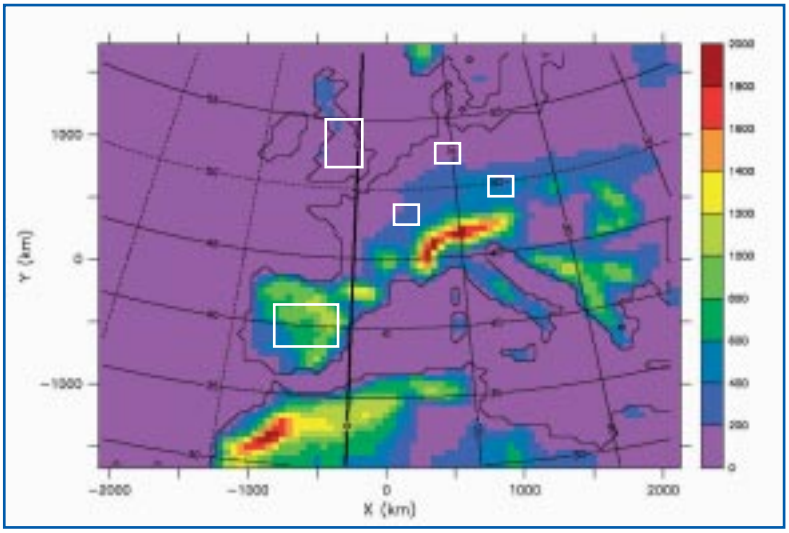

Figure 1: *MAR-domain. Colour shading represents the altitude (in m) of the different grid points in the MAR model. White boxes delimit the different European regions of interest in the BIOCLIM project (see section 4)*

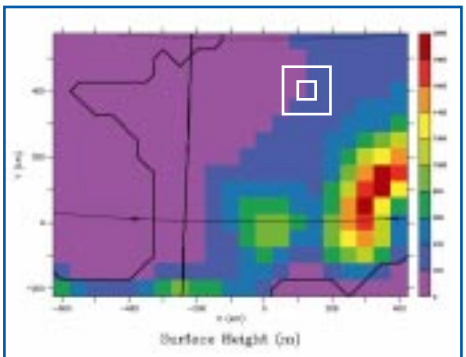

France: *9 grid boxes*
49.0°N - 5.1°E (upper left)
48.1°N - 6.4°E (lower right)

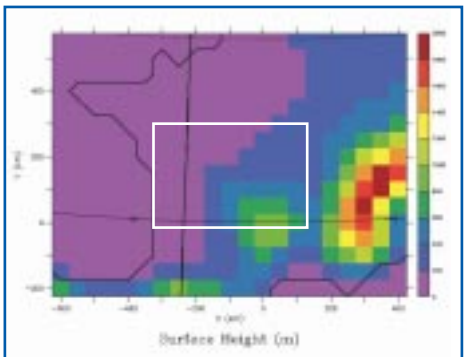

Spain: *63 grid boxes*
41.0°N - 6.5°W (upper left)
38.6°N - 1.6°W (lower right)

Figure 2: *Delimitation of the different European regions of interest in the framework of BIOCLIM.*

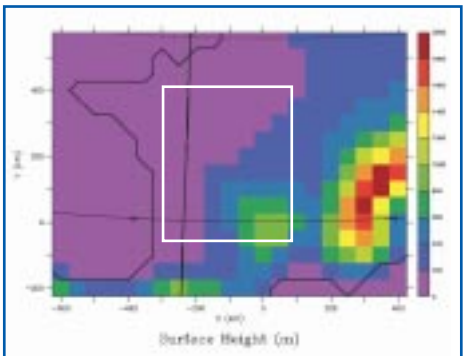

C. England: *40 grid boxes*
54.7°N - 3.2°W (upper left)
51.7°N - 0.1°E (lower right)

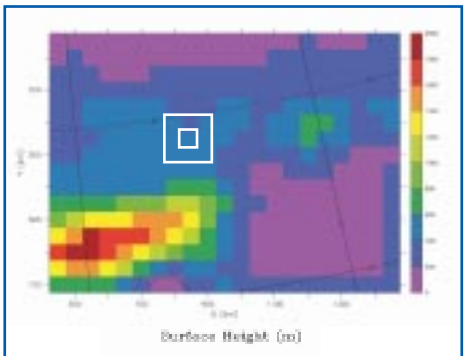

Czech R.: *9 grid boxes*
49.8°N - 14.8°E (upper left)
48.8°N - 16.0°E (lower right)

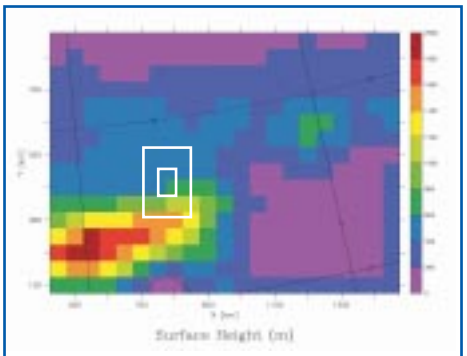

Germany.: *9 grid boxes*
52.9°N - 9.7°E (upper left)
51.9°N - 11.0°E (lower right)

Figures 5-13 for D6: *(a) Surface temperature (K) in DJF, and in (b) JJA. (c) Total precipitation (mm.day^{1}) in DJF, and in (d) JJA. (top left) 30-yr average as simulated by the IPSL_CM4_D model [Ref.1] interpolated on the MAR grid; (top right) the IPSL_CM4_D simulated climate (on the MAR grid) used as boundary condition in the MAR simulation; (bottom left) the MAR simulated climate; (bottom right) adjusted field (see text).*

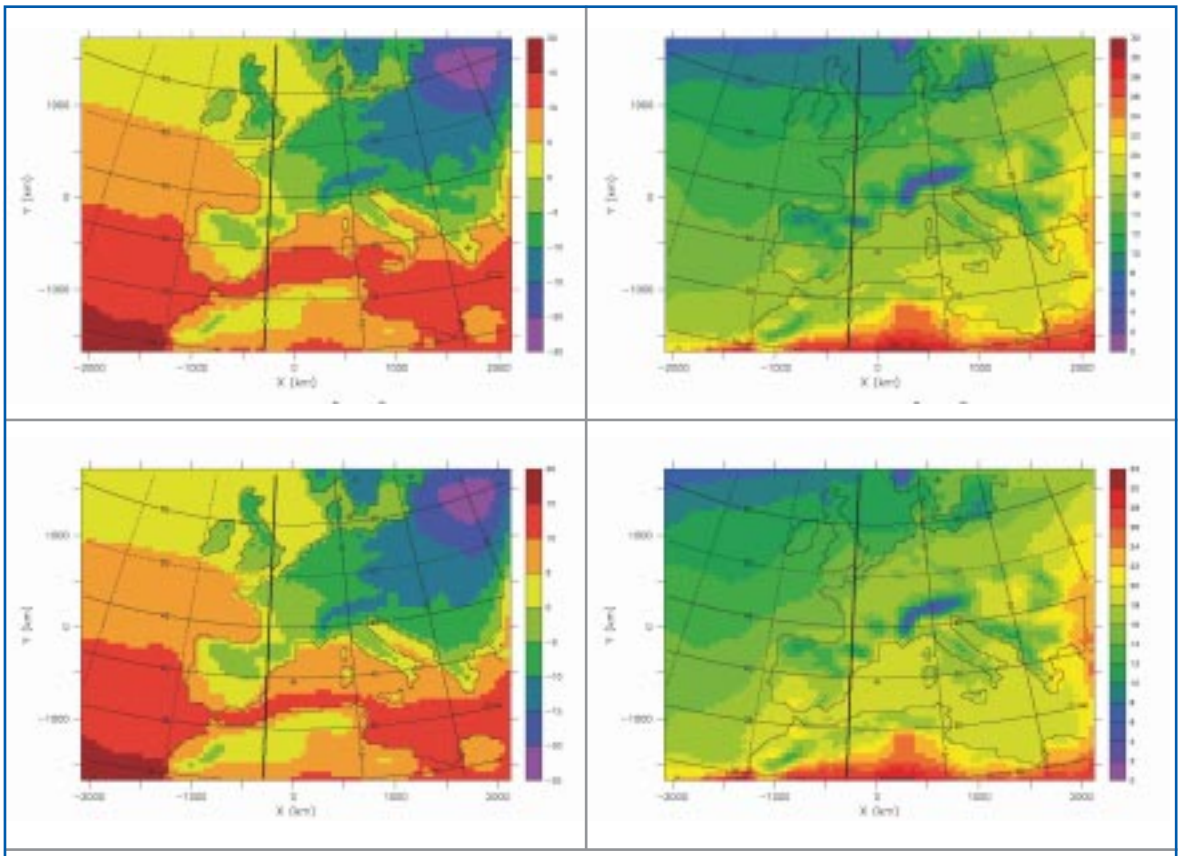

Figure 3a : *Baseline simulation - Surface temperature DJF (top left) and JJA (top right) simulated by MAR in the baseline experiment. The adjusted surface temperature field (DJF (bottom left) and JJA (bottom right)).*

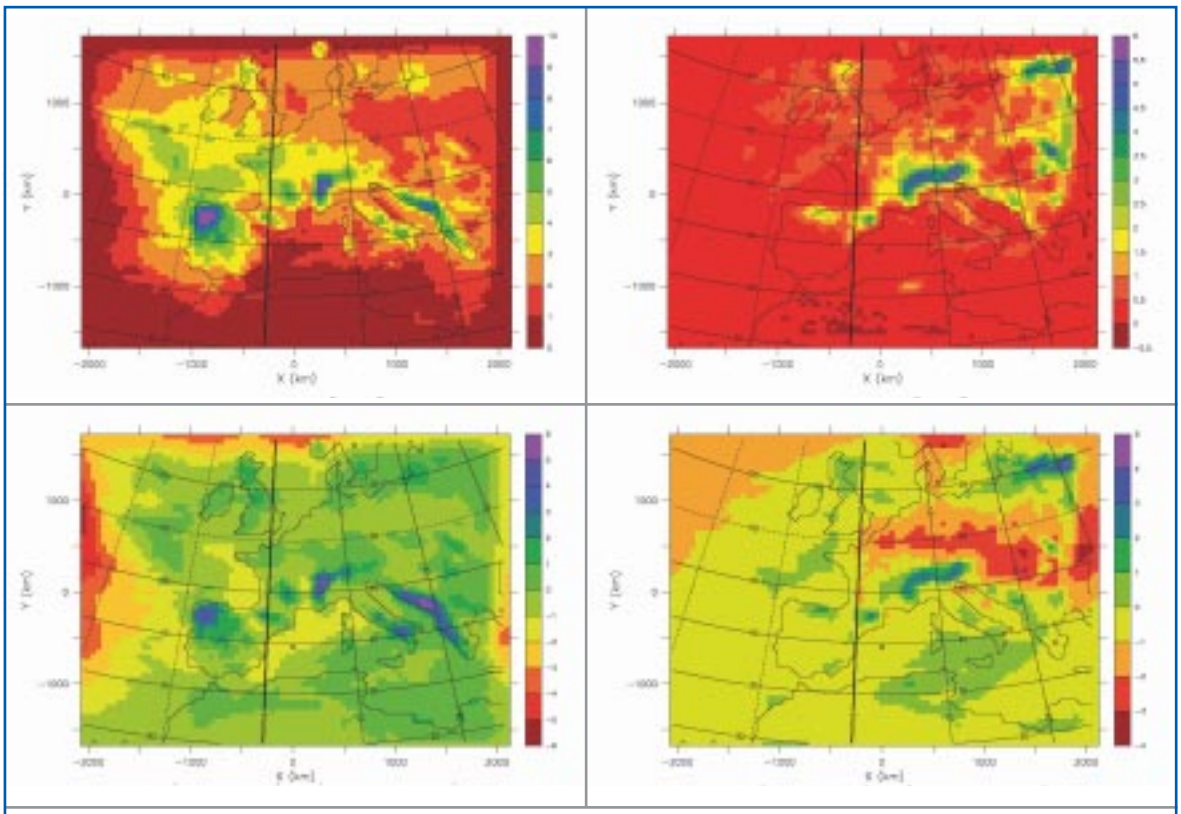

Figure 3b : *Baseline simulation - Total precipitation DJF (top left) and JJA (top right) simulated by MAR in the baseline experiment. The adjusted precipitation field (DJF (bottom left) and JJA (bottom right)).*

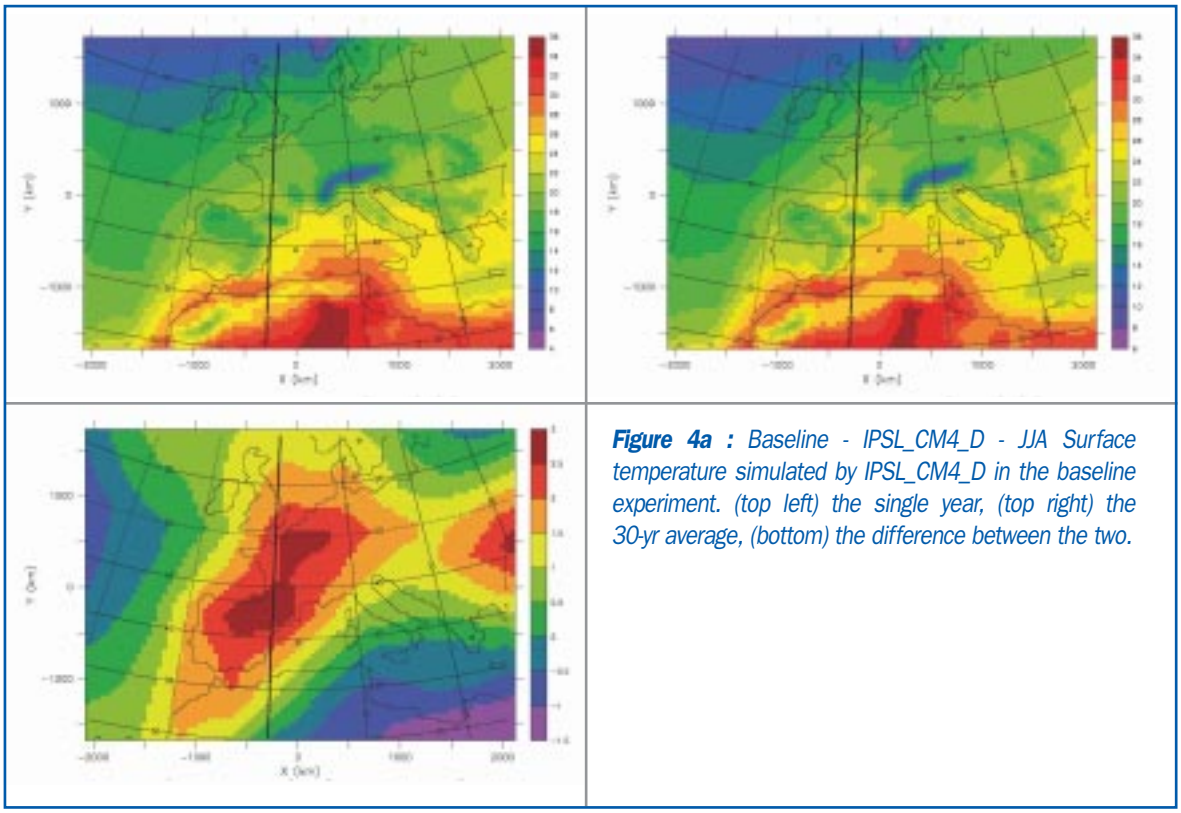

Figure 4a : *Baseline - IPSL_CM4_D - JJA Surface temperature simulated by IPSL_CM4_D in the baseline experiment. (top left) the single year, (top right) the 30-yr average, (bottom) the difference between the two.*

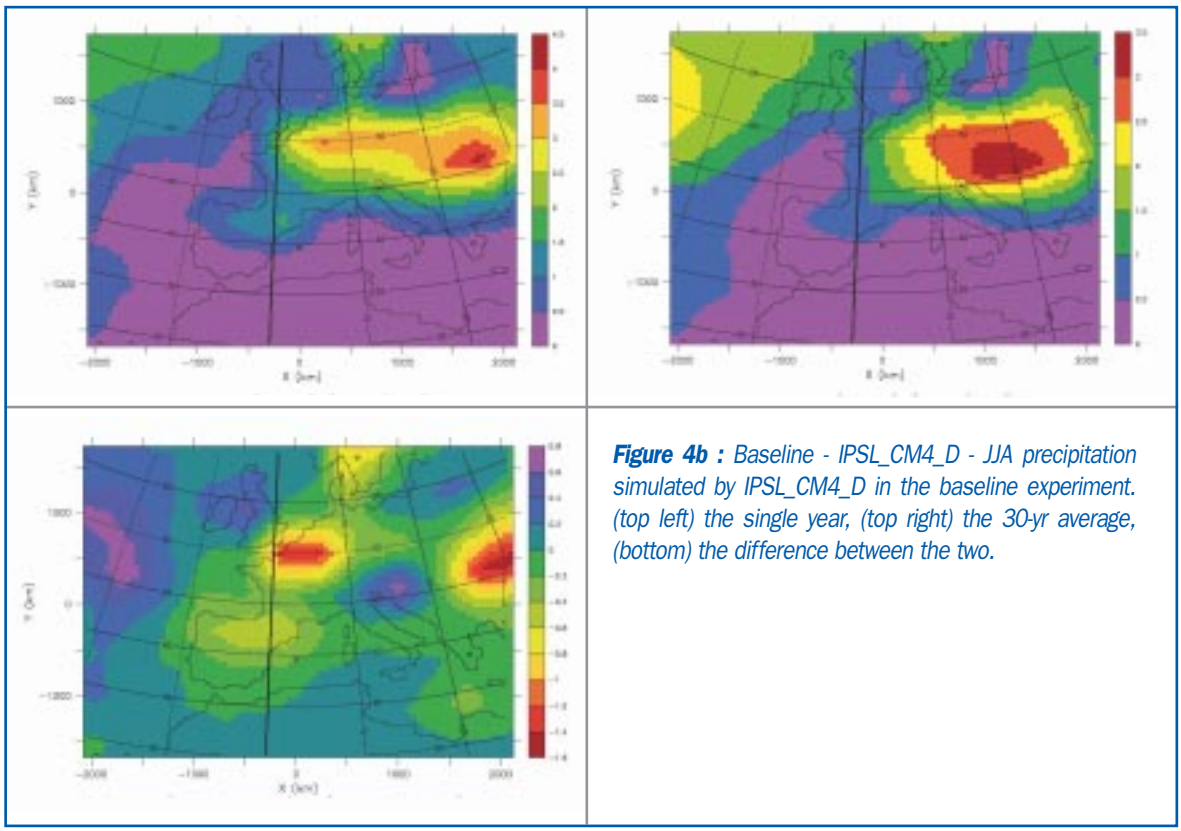

Figure 4b : *Baseline - IPSL_CM4_D - JJA precipitation simulated by IPSL_CM4_D in the baseline experiment. (top left) the single year, (top right) the 30-yr average, (bottom) the difference between the two.*

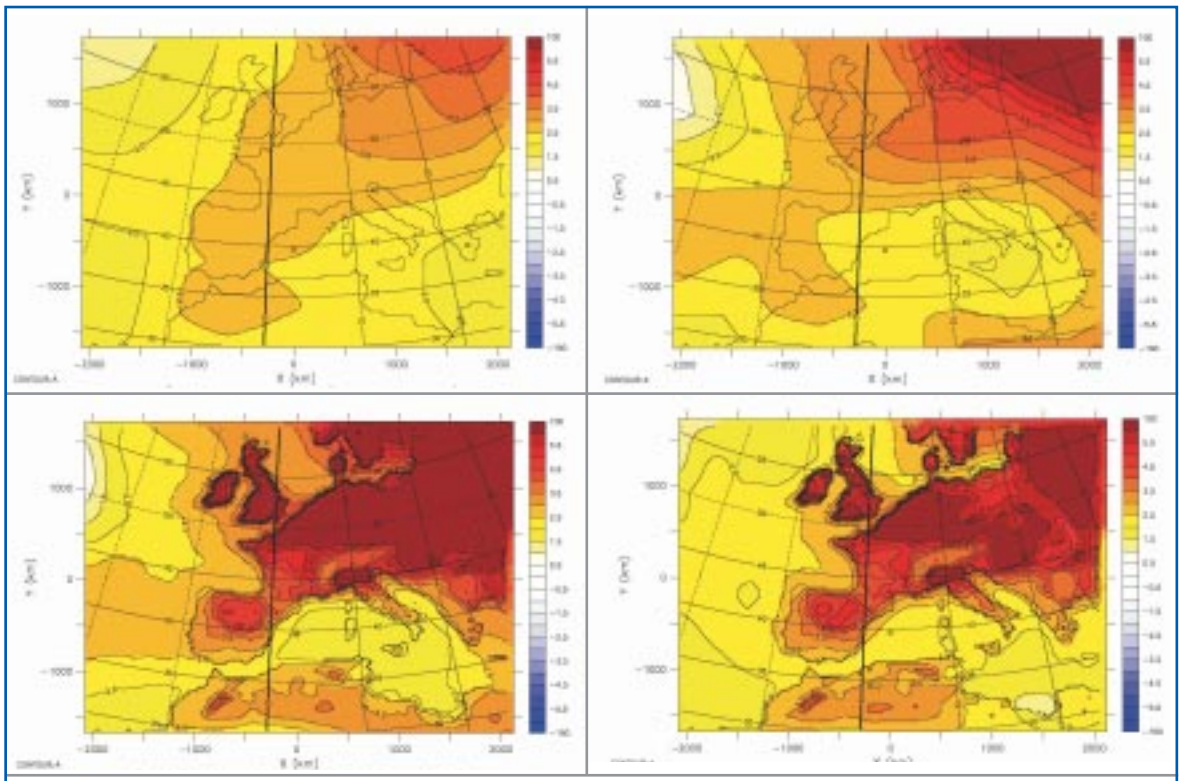

Figure 5a: *"A"– Baseline. Surface temperature DJF anomalies of experiments "A" minus control.*

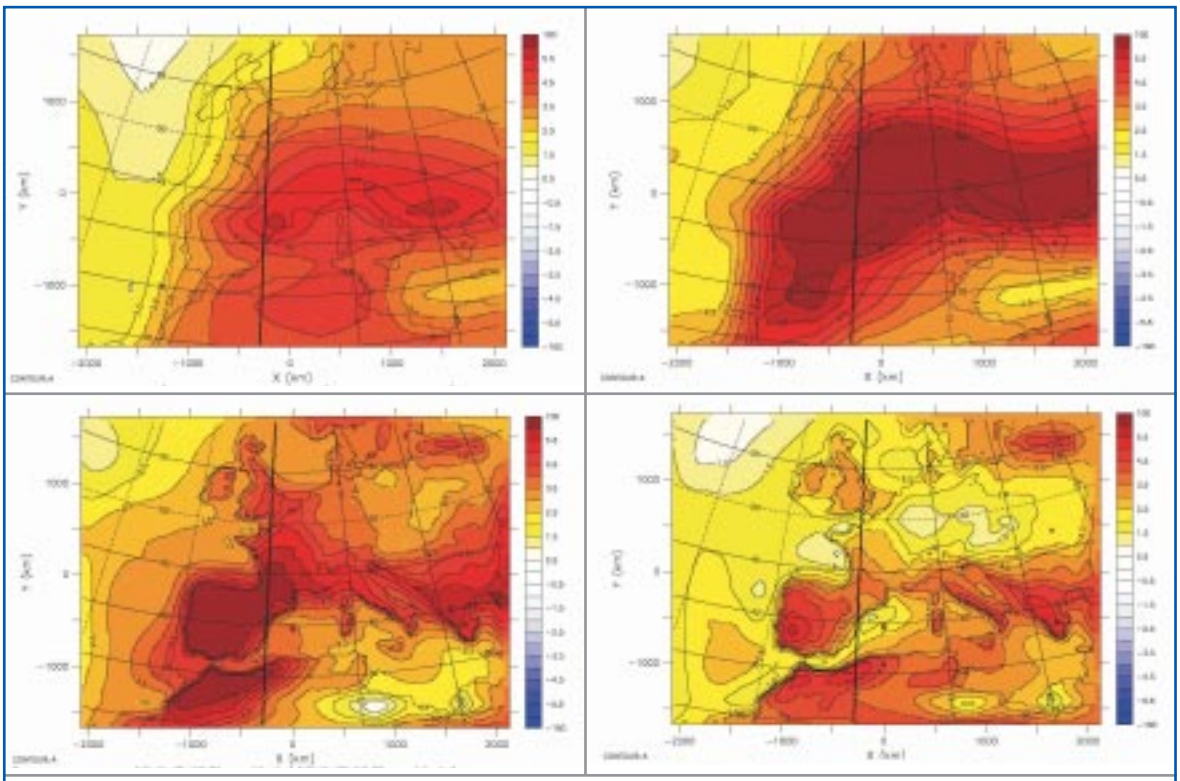

Figure 5b : *"A"– Baseline. Surface temperature JJA anomalies of experiments "A" minus control.*

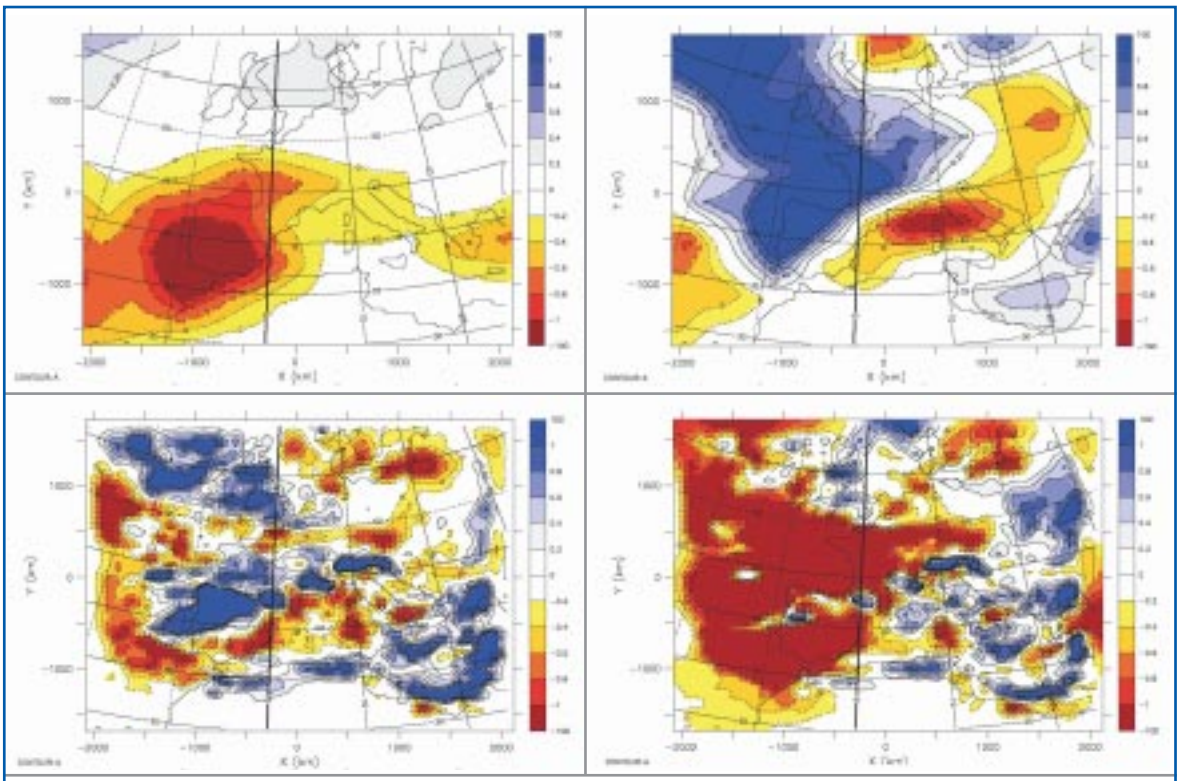

Figure 5c : *"A"– Baseline. Total precipitation DJF anomalies of experiments "A" minus control.*

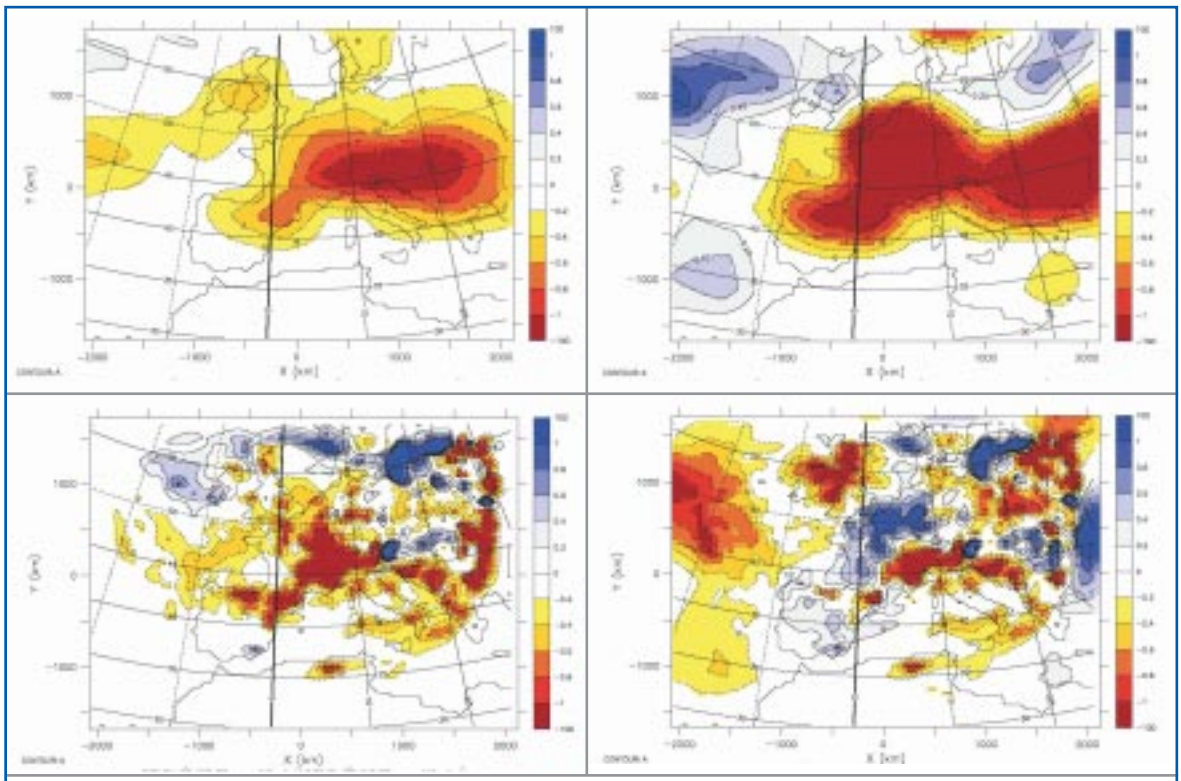

Figure 5d: *"A"– Baseline. Total precipitation JJA anomalies of experiments "A" minus control.*

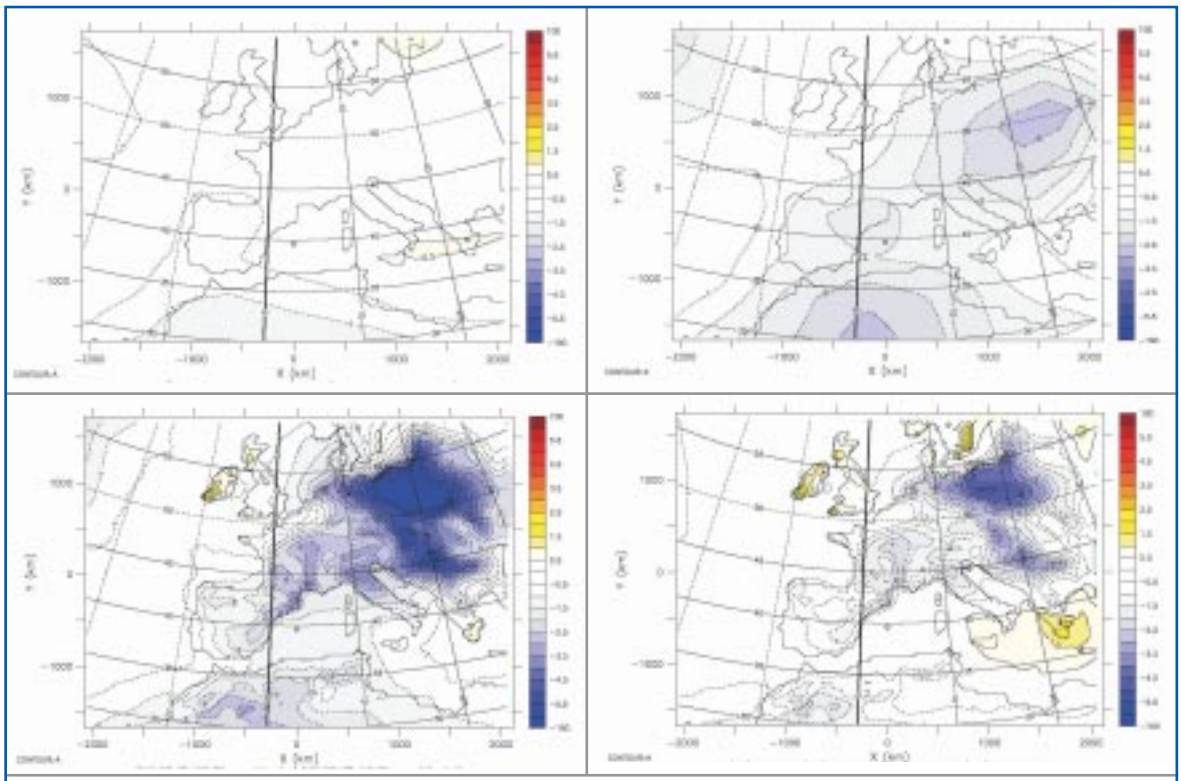

Figure 6a: *"E"– Baseline. Surface temperature DJF anomalies of experiments "E" minus control.*

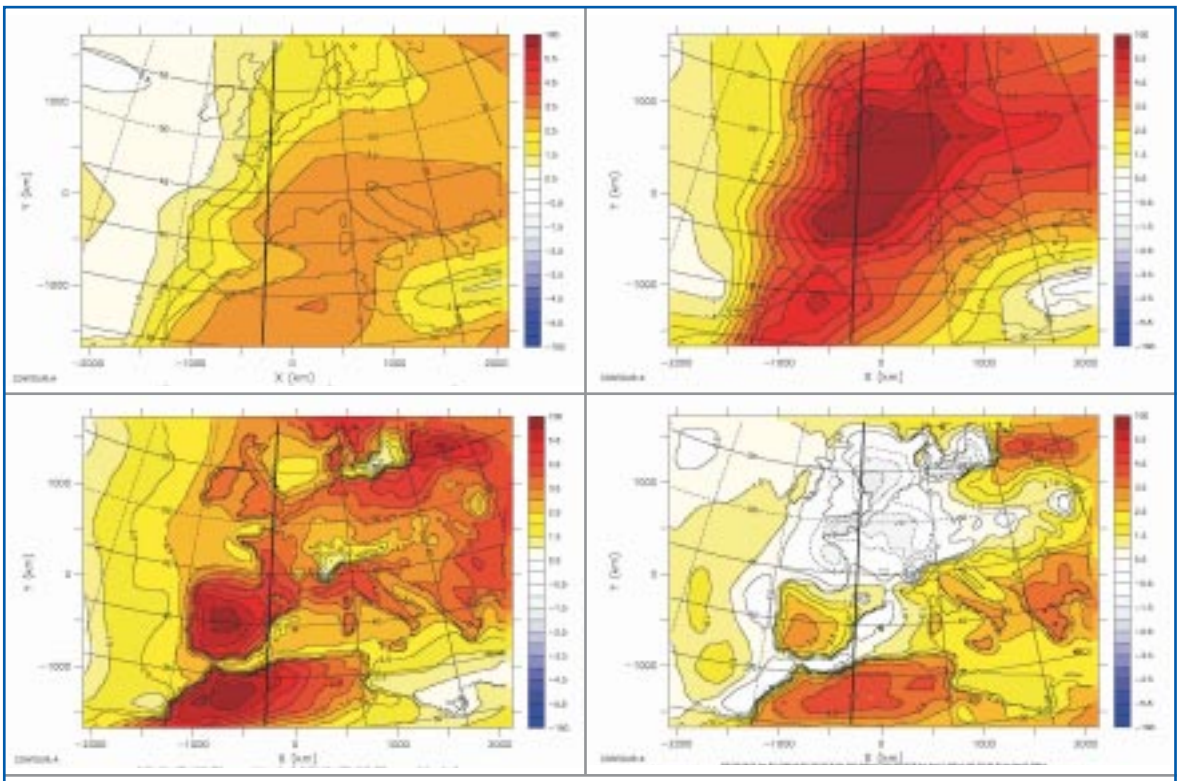

Figure 6b: *"E"– Baseline. Surface temperature JJA anomalies of experiments "E" minus control.*

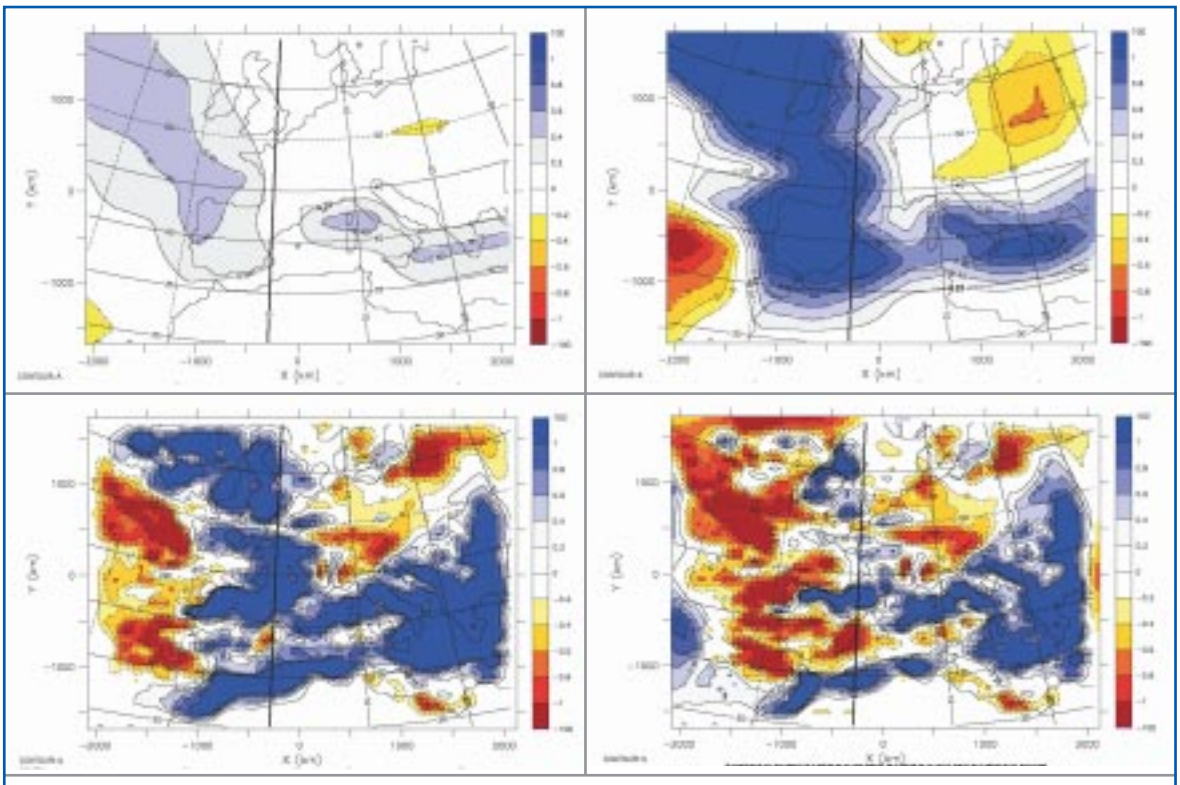

Figure 6c: *"E"– Baseline. Total precipitation DJF anomalies of experiments "E" minus control.*

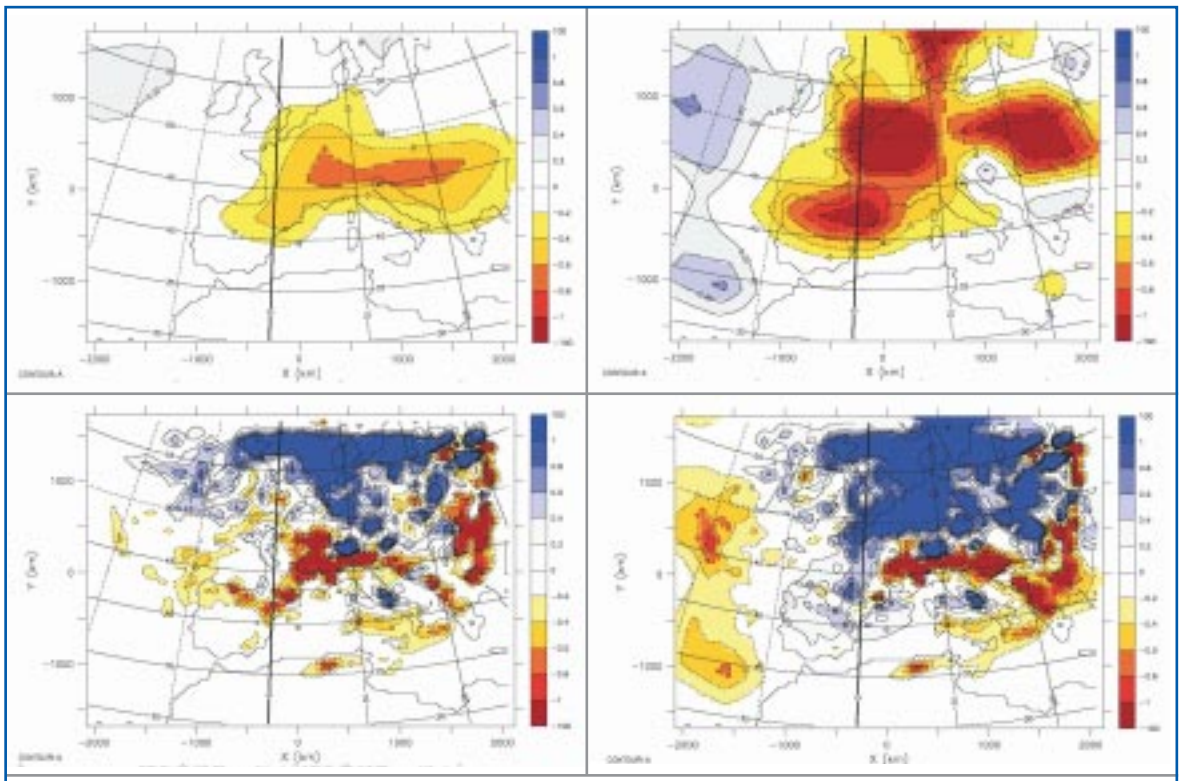

Figure 6d: *"E"– Baseline. Total precipitation JJA anomalies of experiments "E" minus control.*

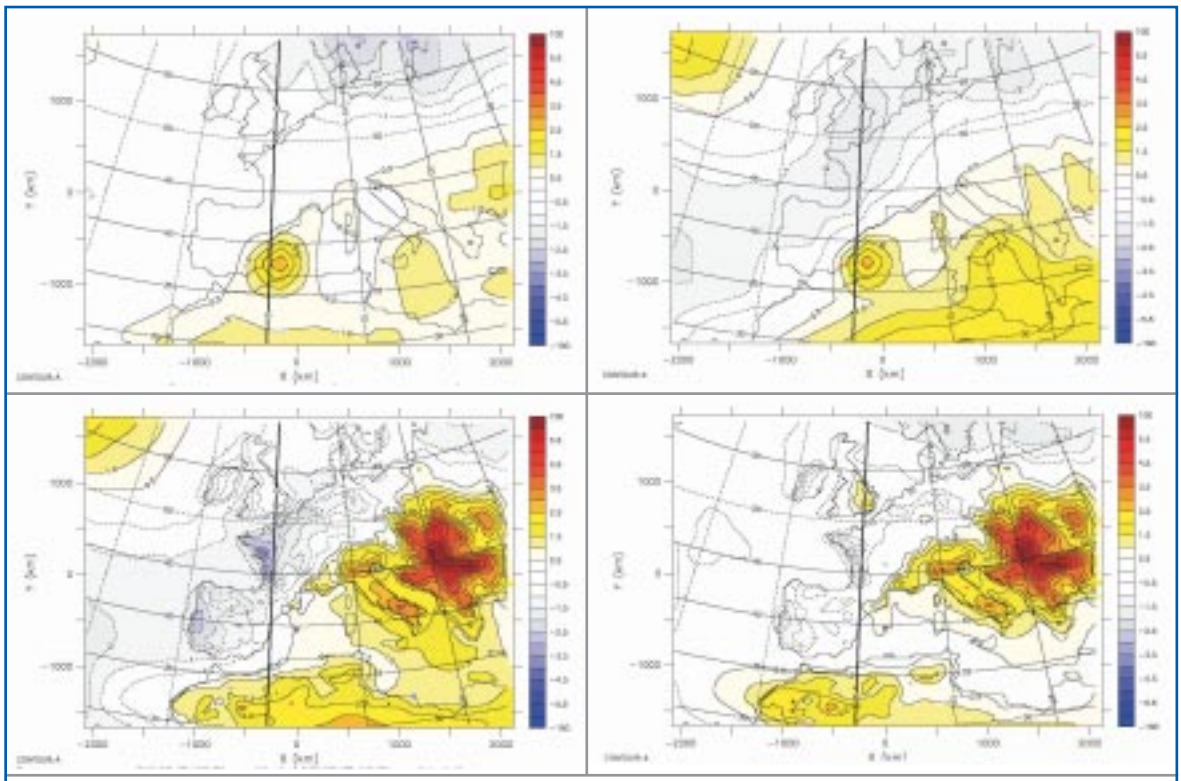

Figure 7a: *"D"—"E". Surface temperature DJF anomalies of experiments "D" minus "E".*

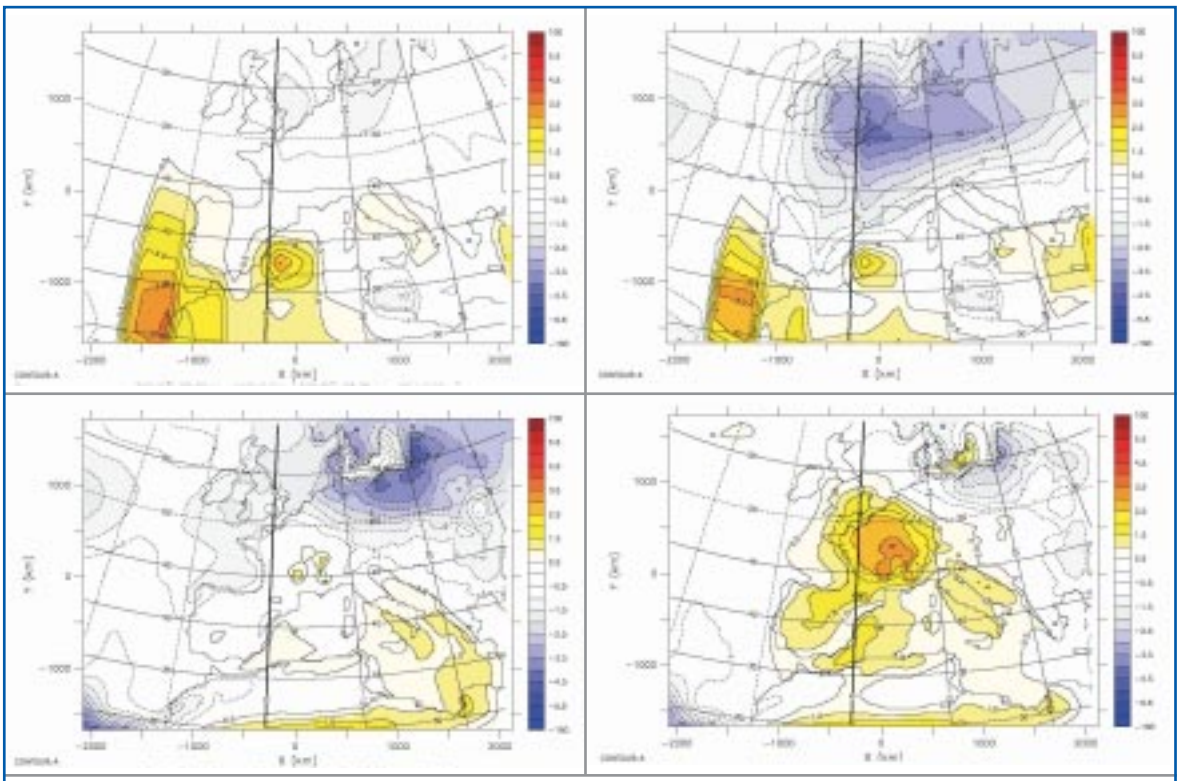

Figure 7b: *"D"—"E". Surface temperature JJA anomalies of experiments "D" minus "E".*

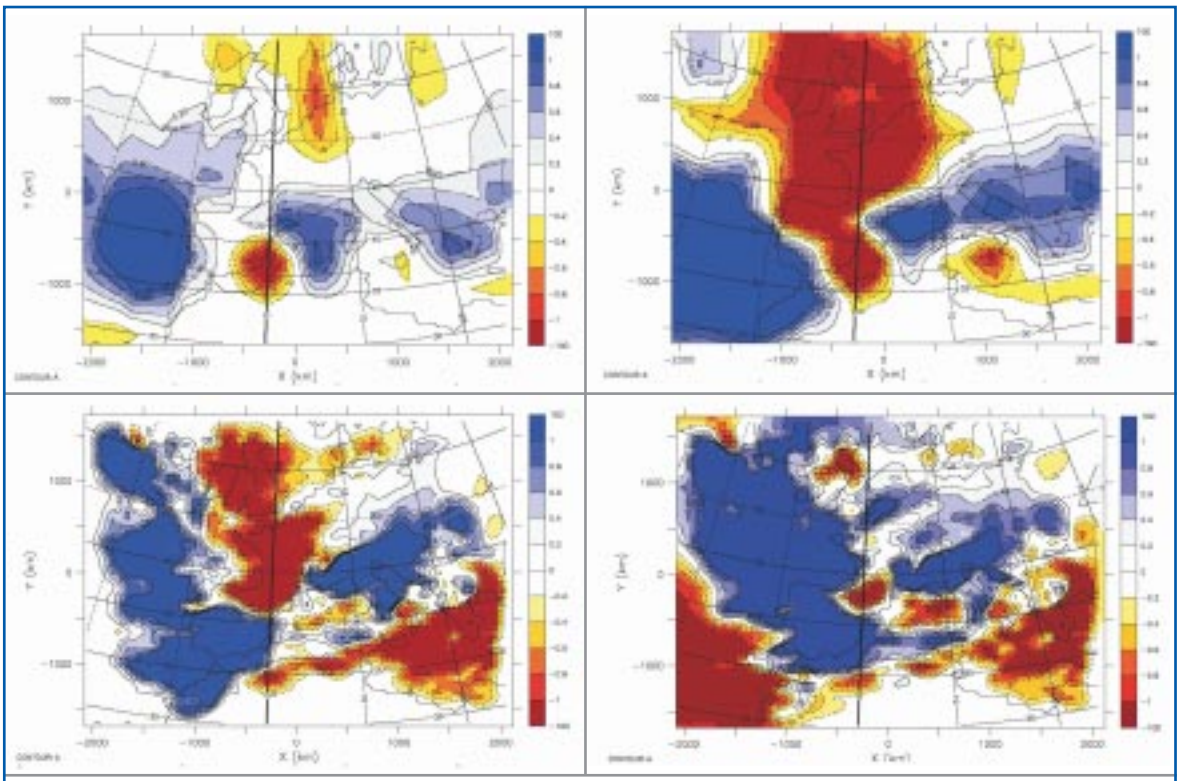

Figure 7c: *"D"—"E". Total precipitation DJF anomalies of experiments "D" minus "E".*

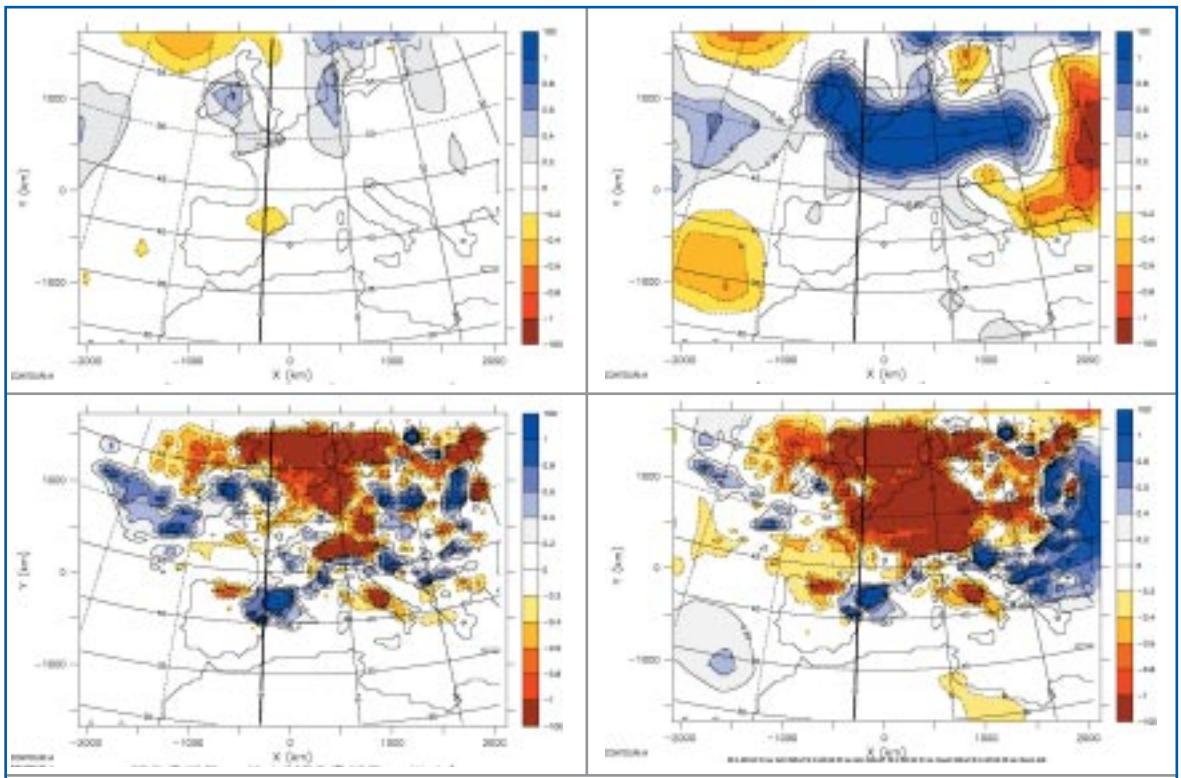

Figure 7d: *"D"—"E". Total precipitation JJA anomalies of experiments "D" minus "E".*

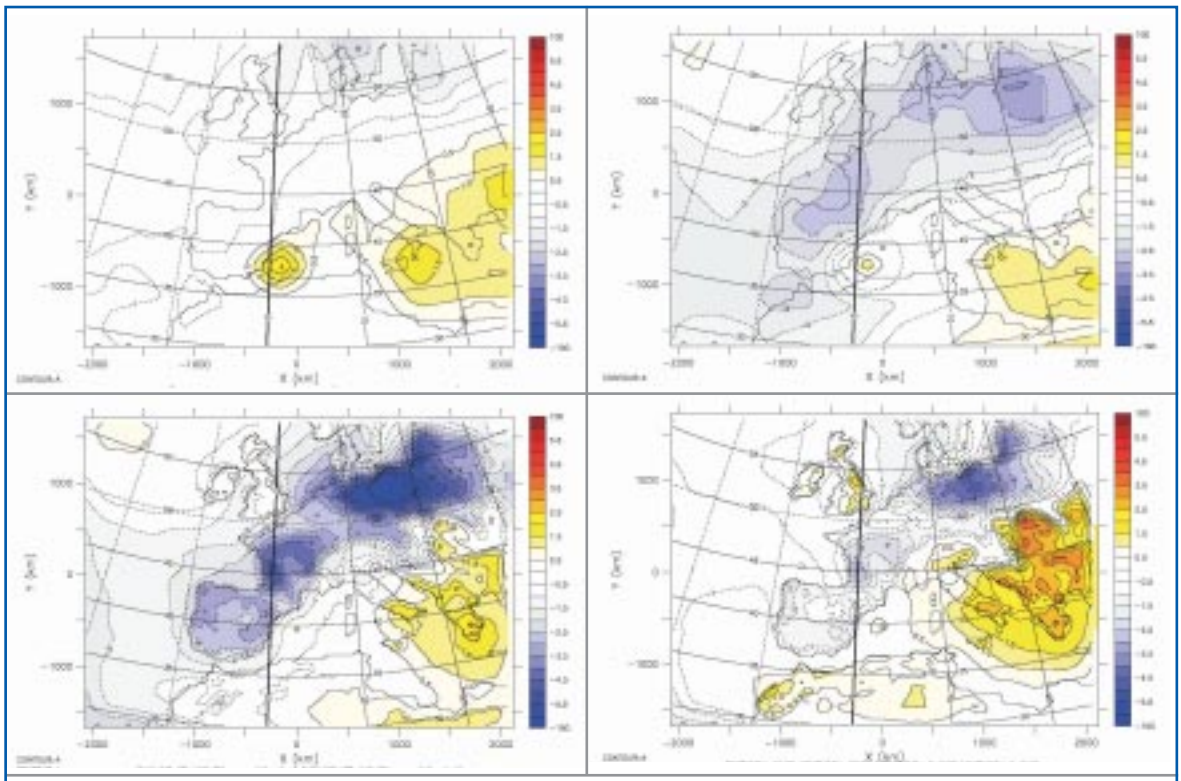

Figure 8a: *"D"- Baseline. Surface temperature DJF anomalies of experiments "D" minus control.*

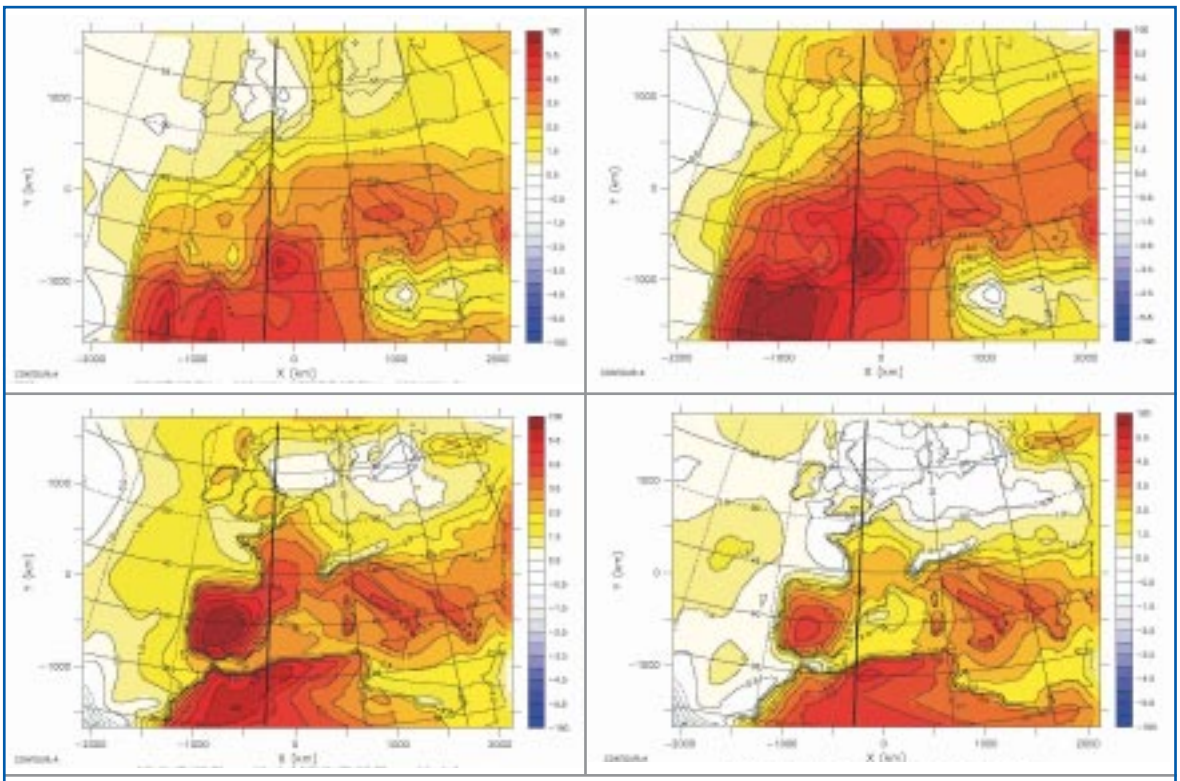

Figure 8b: *"D"- Baseline. Surface temperature JJA anomalies of experiments "D" minus control.*

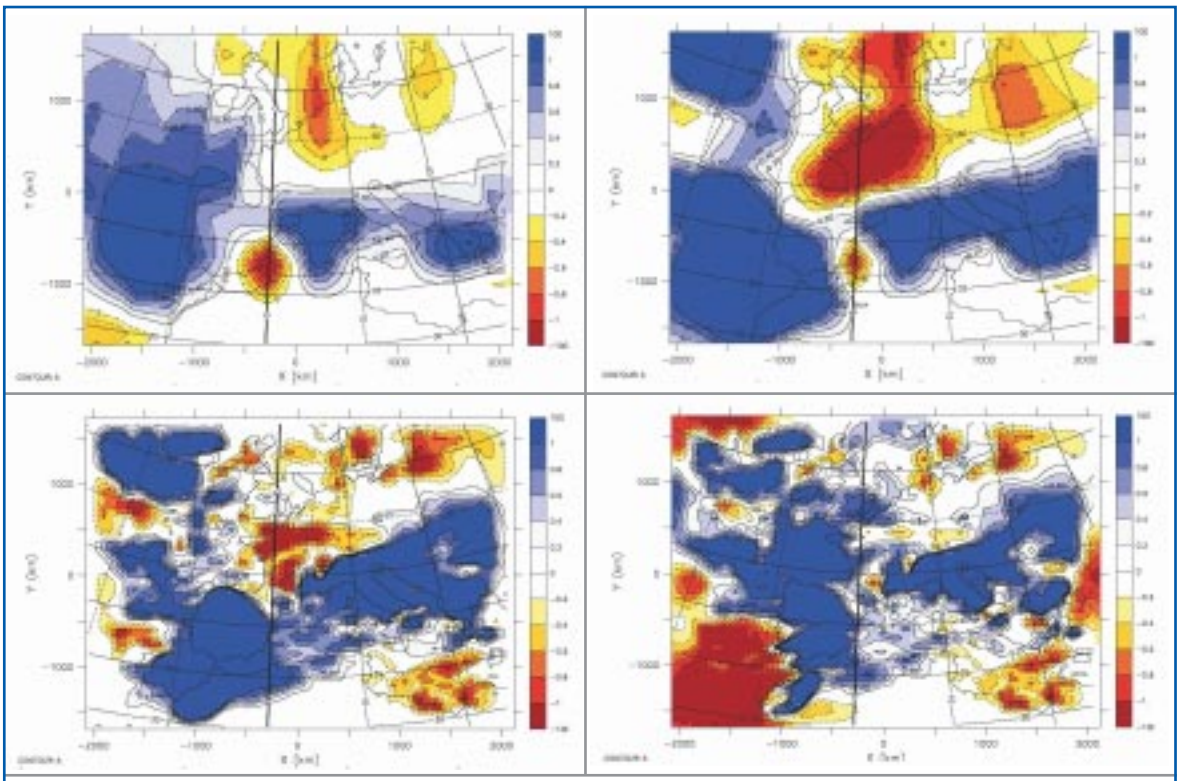

Figure 8c: *"D"- Baseline. Total precipitation DJF anomalies of experiments "D" minus control.*

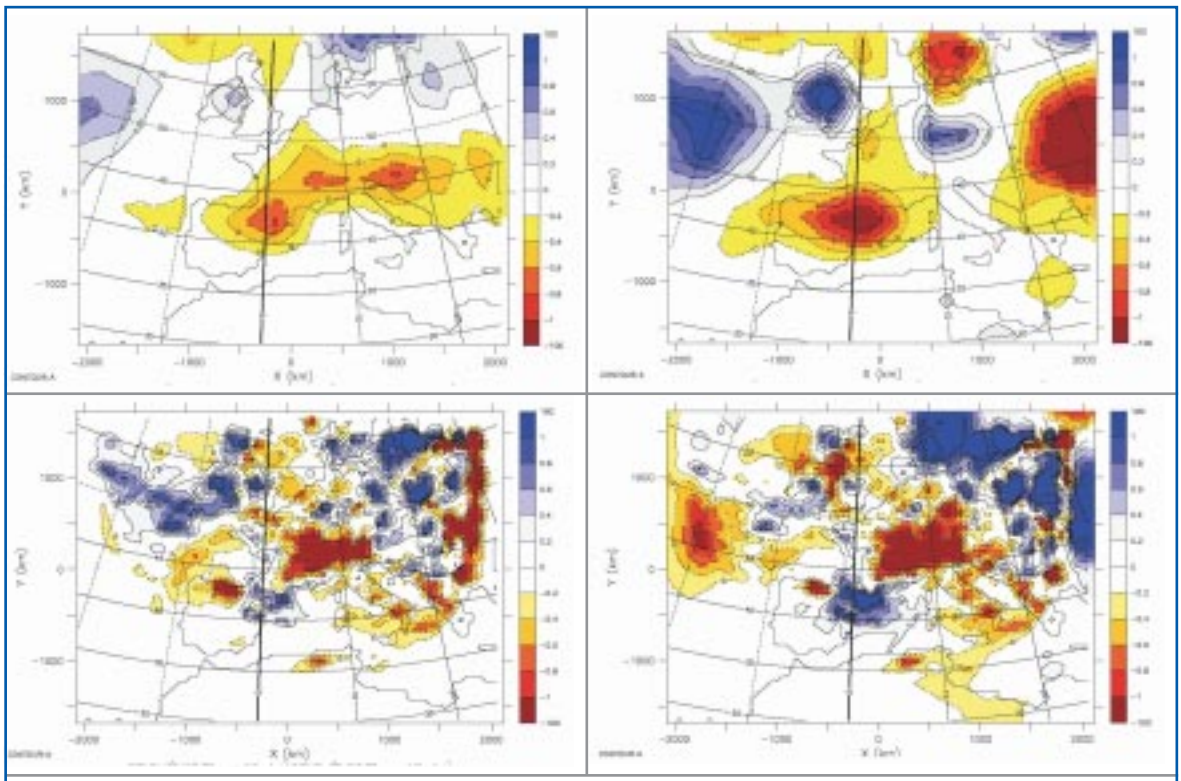

Figure 8d: *"D"- Baseline. Total precipitation JJA anomalies of experiments "D" minus control.*

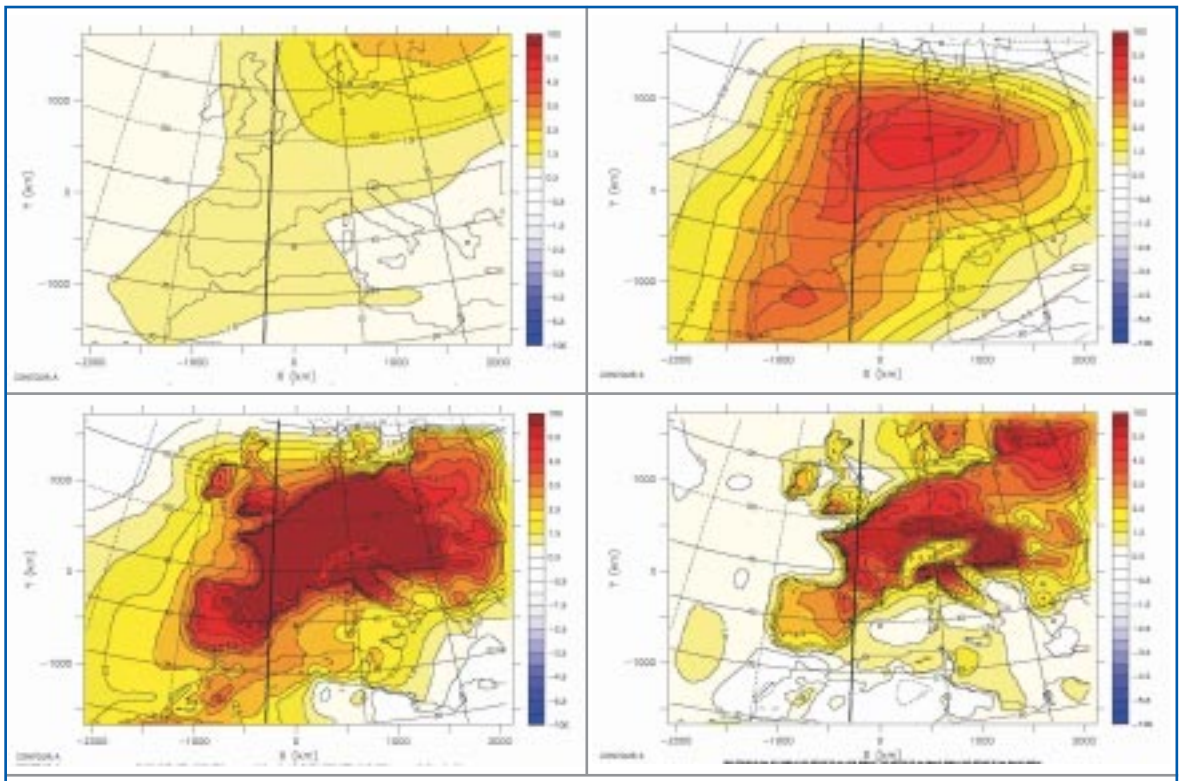

Figure 9a: *"C"–"D". Surface temperature DJF anomalies of experiments "C" minus "D".*

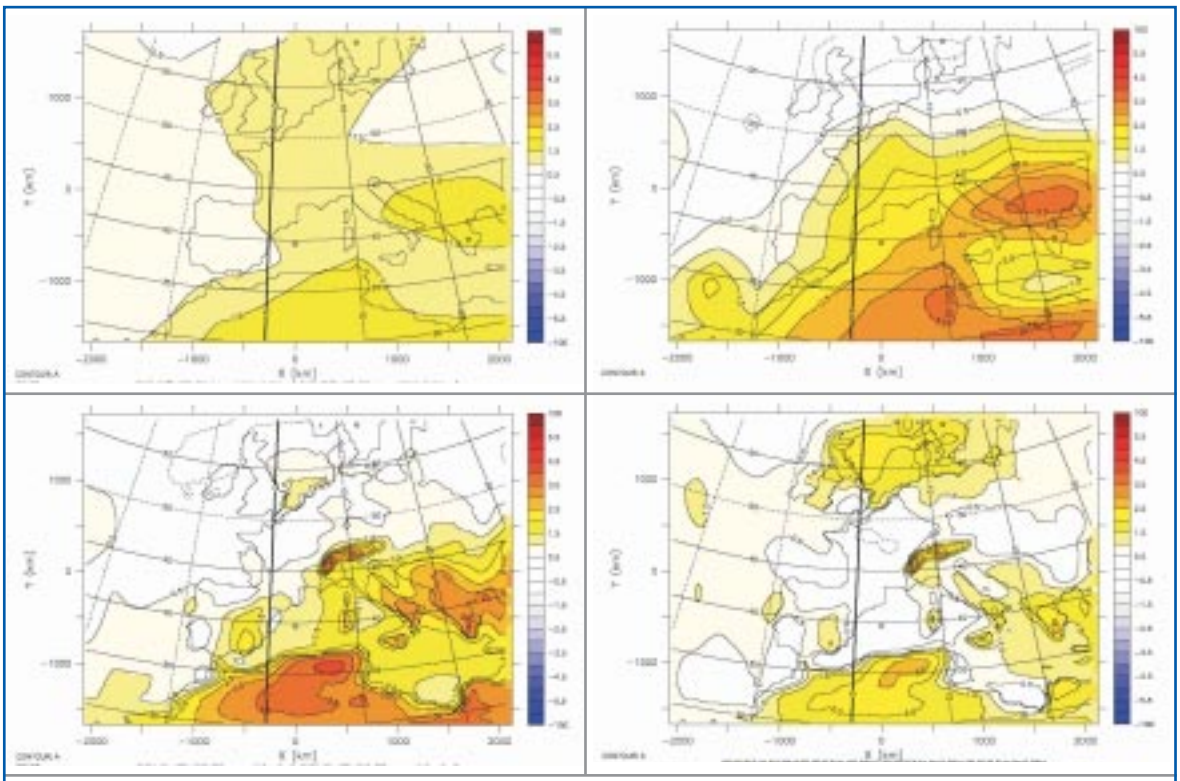

Figure 9b: *"C"–"D". Surface temperature JJA anomalies of experiments "C" minus "D".*

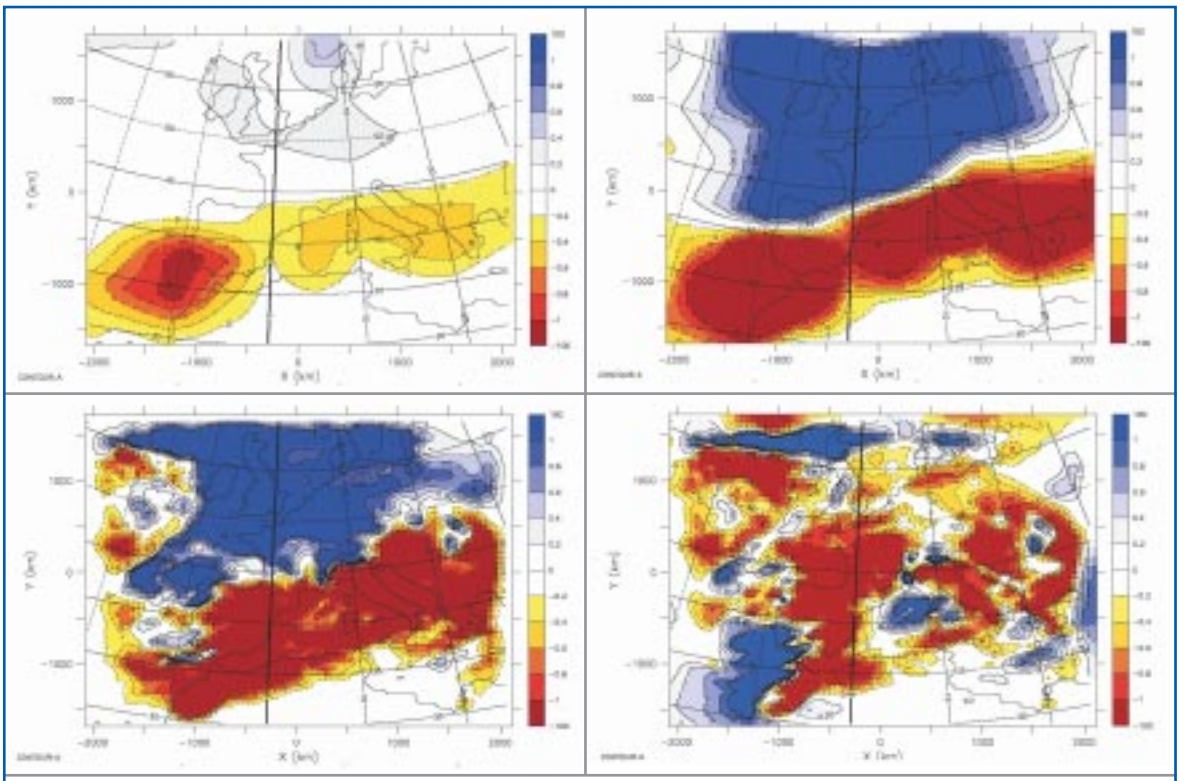

Figure 9c: *"C"–"D". Total precipitation DJF anomalies of experiments "C" minus "D".*

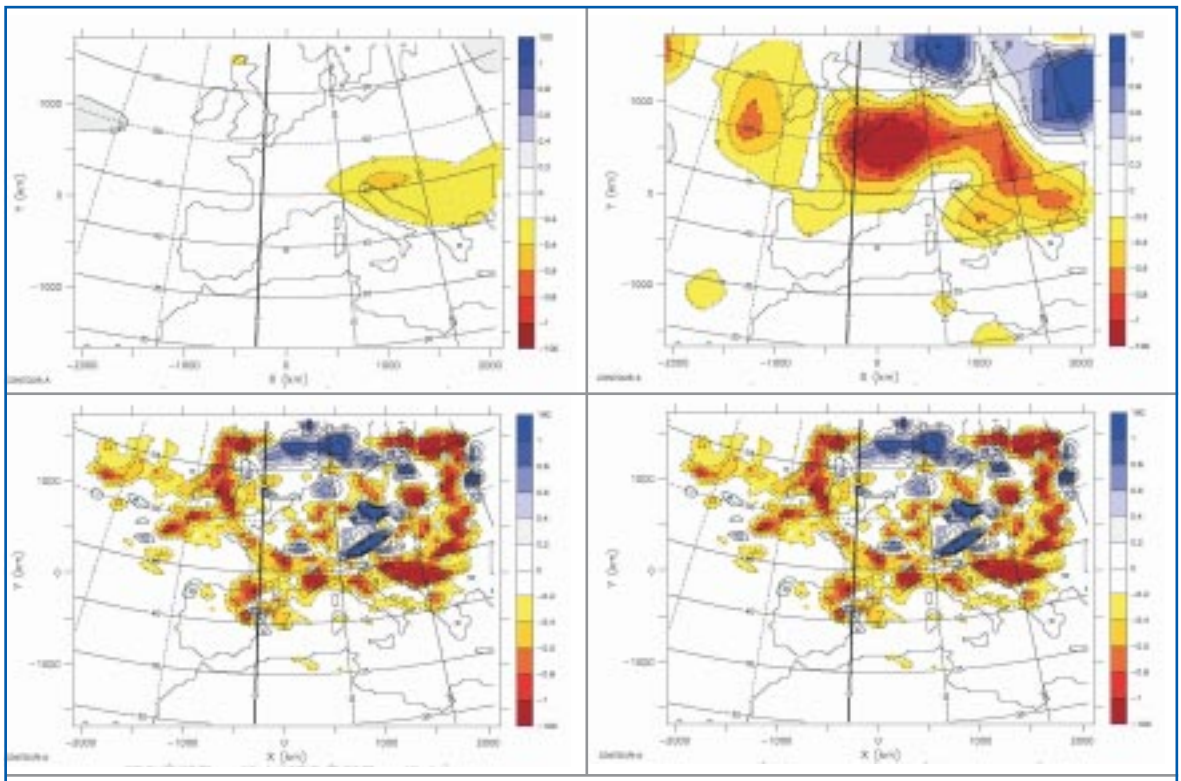

Figure 9d: *"C"–"D". Total precipitation JJA anomalies of experiments "C" minus "D".*

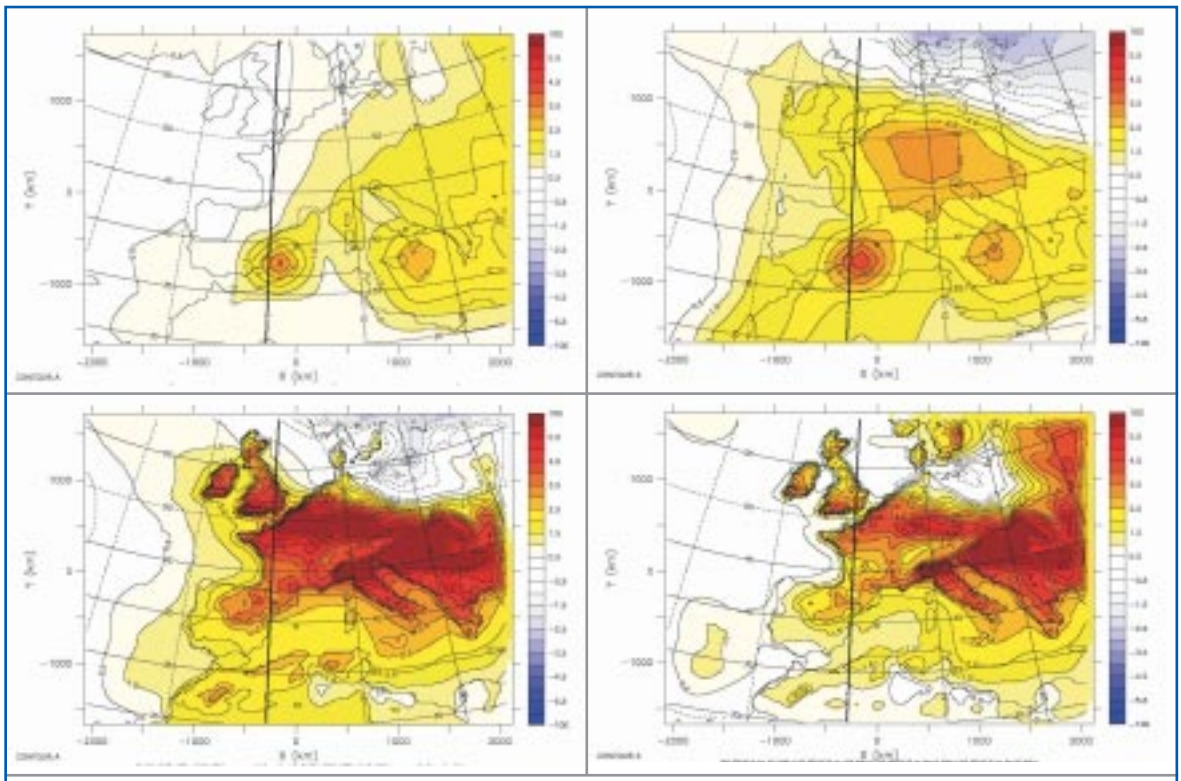

Figure 10a: *"C"–baseline. Surface temperature DJF anomalies of experiments "C" minus control.*

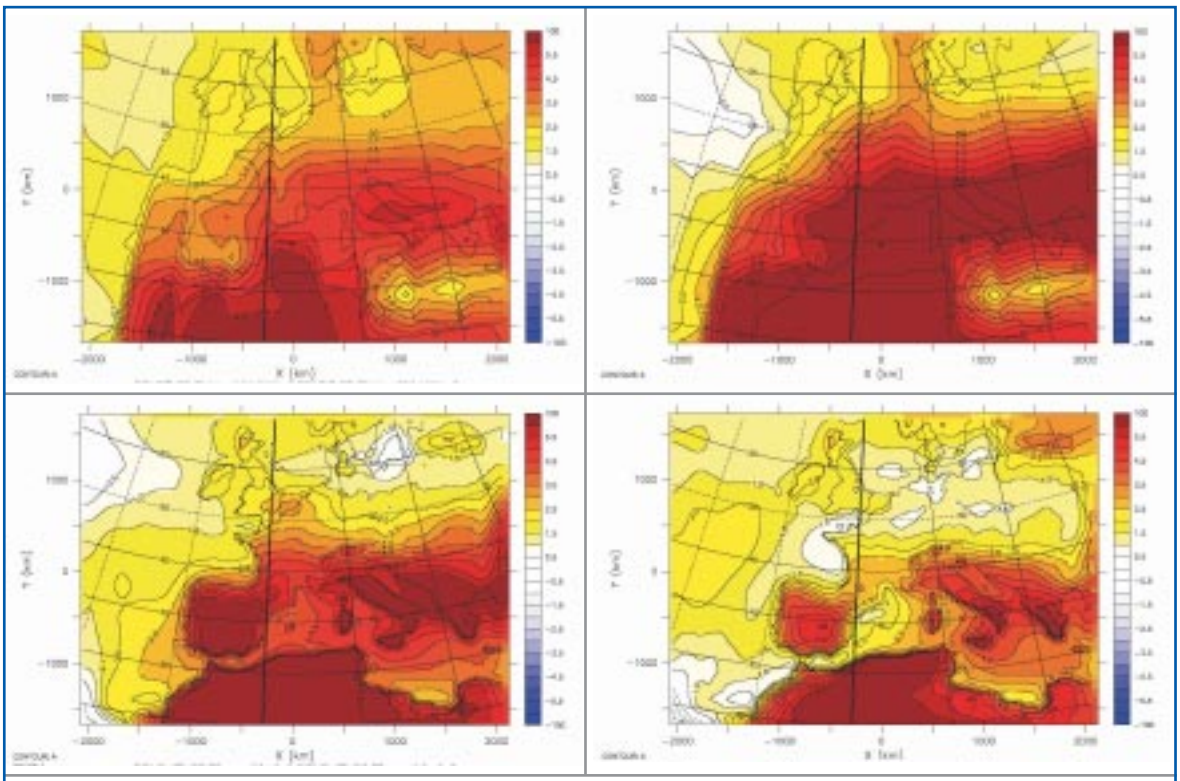

Figure 10b: *"C"– Baseline. Surface temperature JJA anomalies of experiments "C" minus control.*

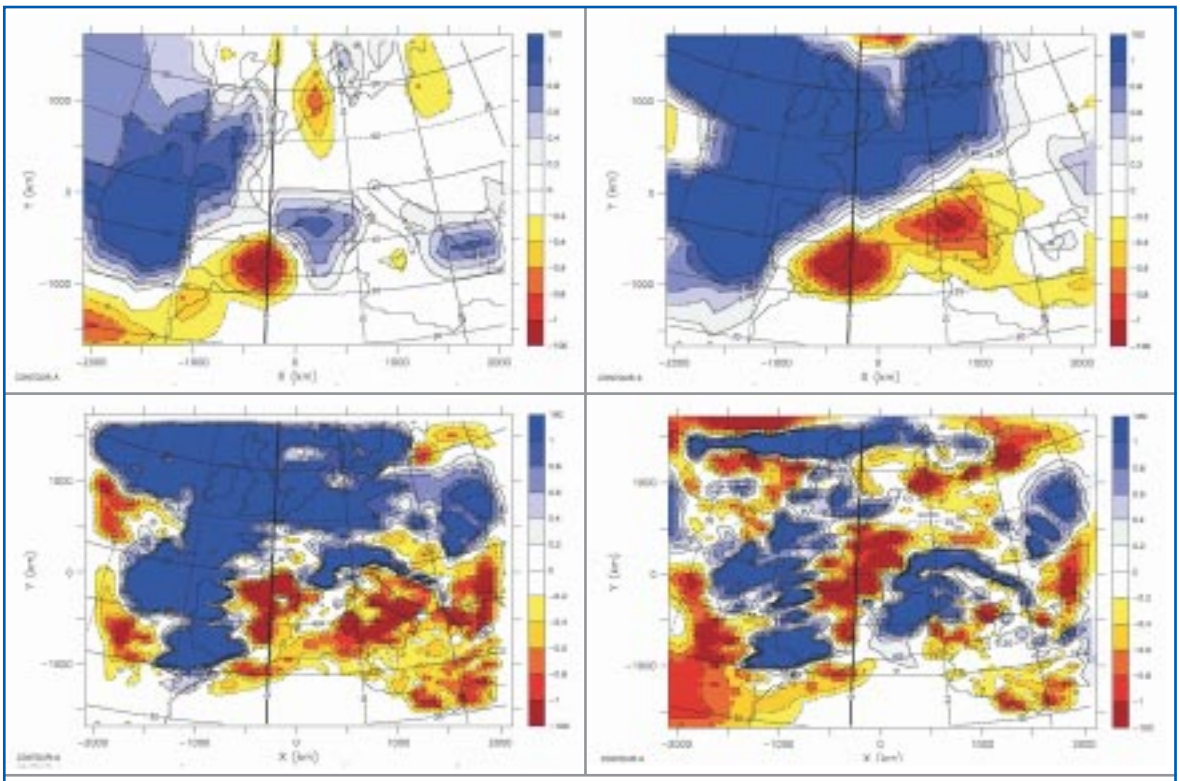

Figure 10c: *"C"– Baseline. Total precipitation DJF anomalies of experiments "C" minus control.*

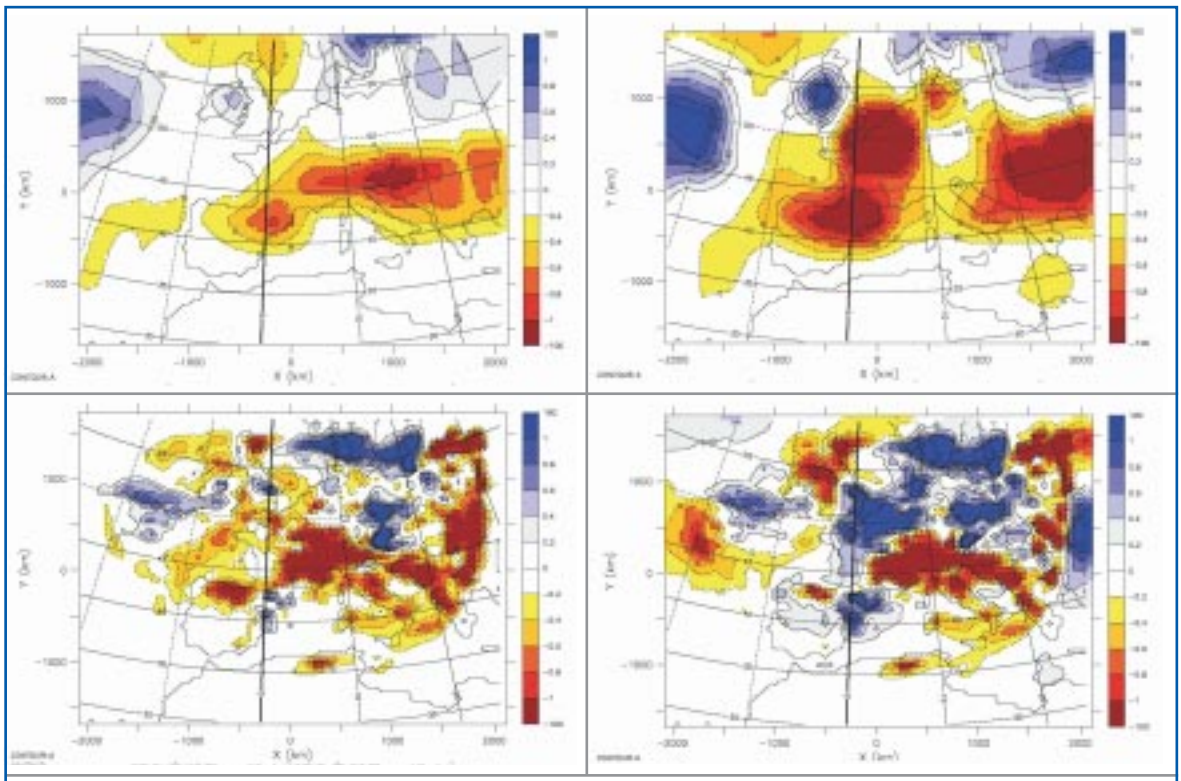

Figure 10d: *"C"– Baseline. Total precipitation JJA anomalies of experiments "C" minus control.*

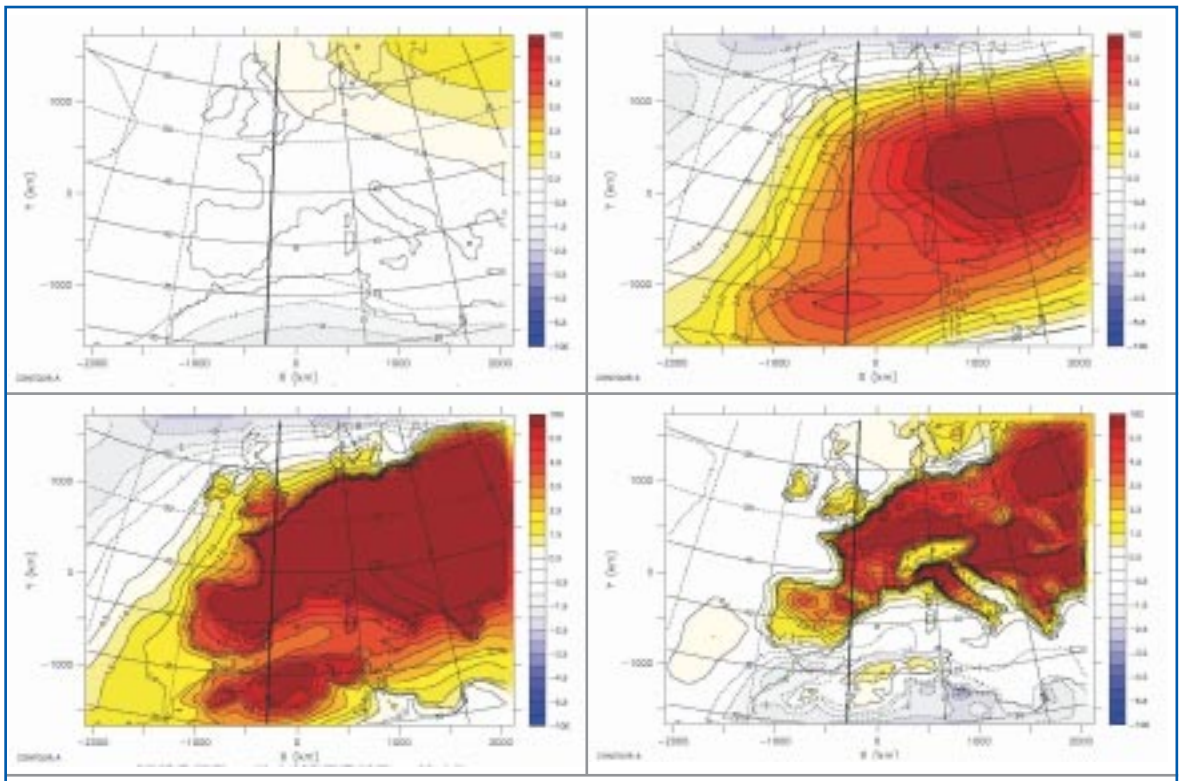

Figure 11a: *"C"–"B". Surface temperature DJF anomalies of experiments "C" minus "B".*

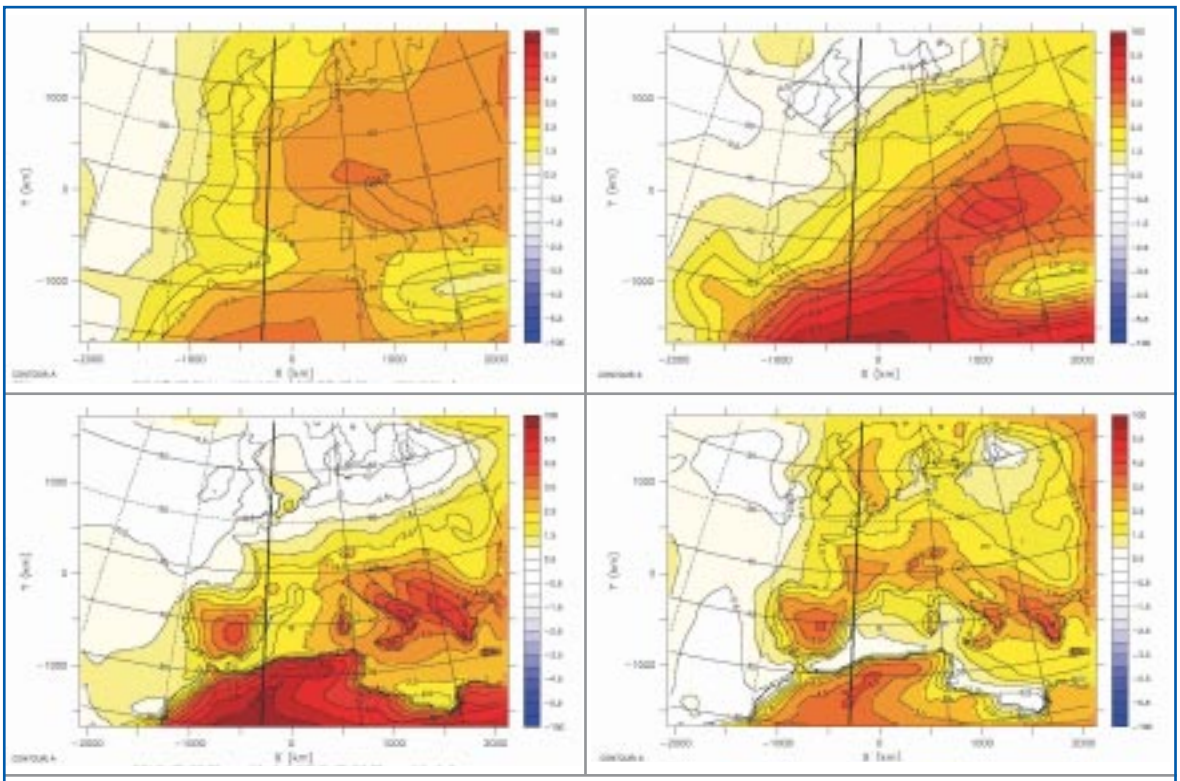

Figure 11b: *"C"–"B". Surface temperature JJA anomalies of experiments "C" minus "B".*

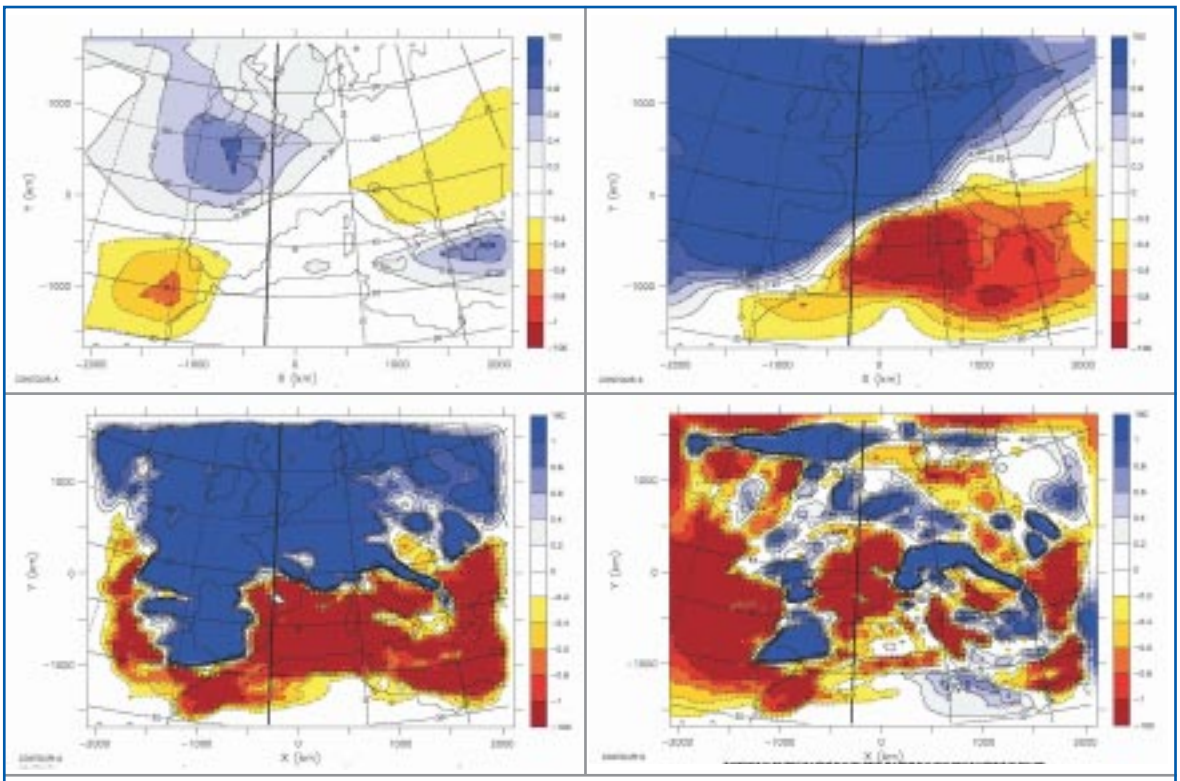

Figure 11c: *"C"–"B". Total precipitation DJF anomalies of experiments "C" minus "B".*

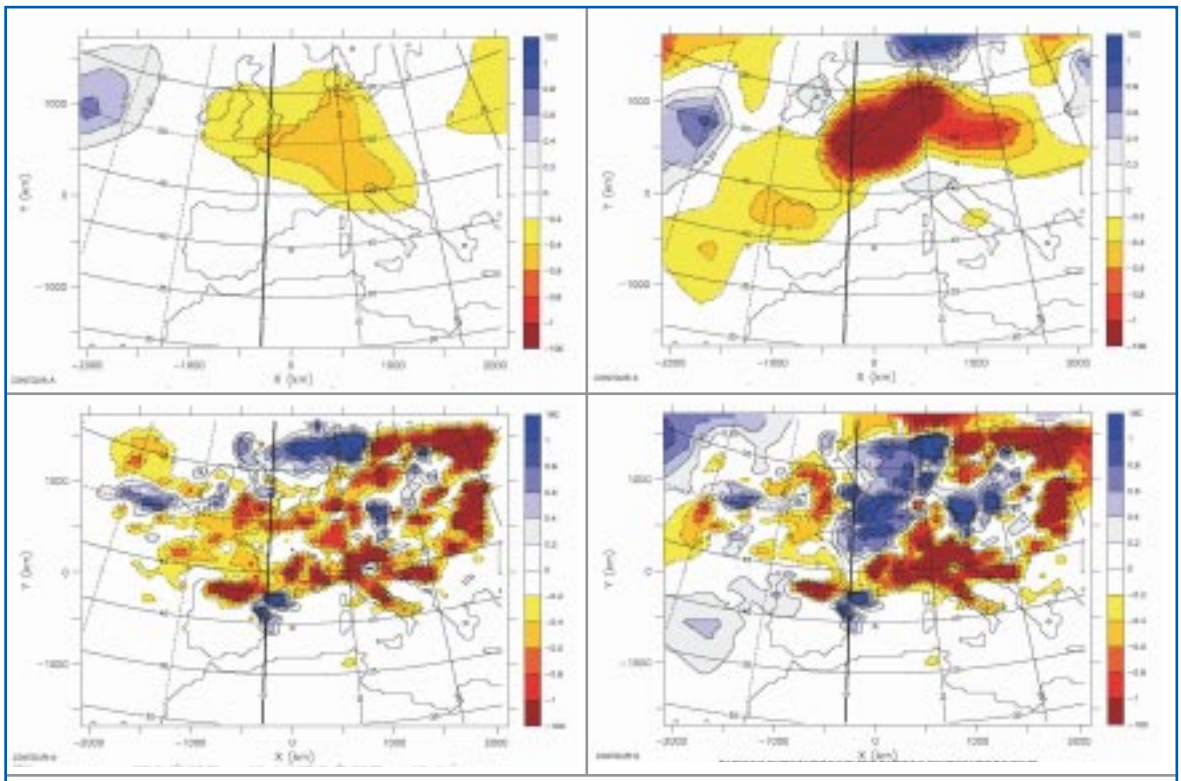

Figure 11d: *"C"–"B". Total precipitation JJA anomalies of experiments "C" minus "B".*

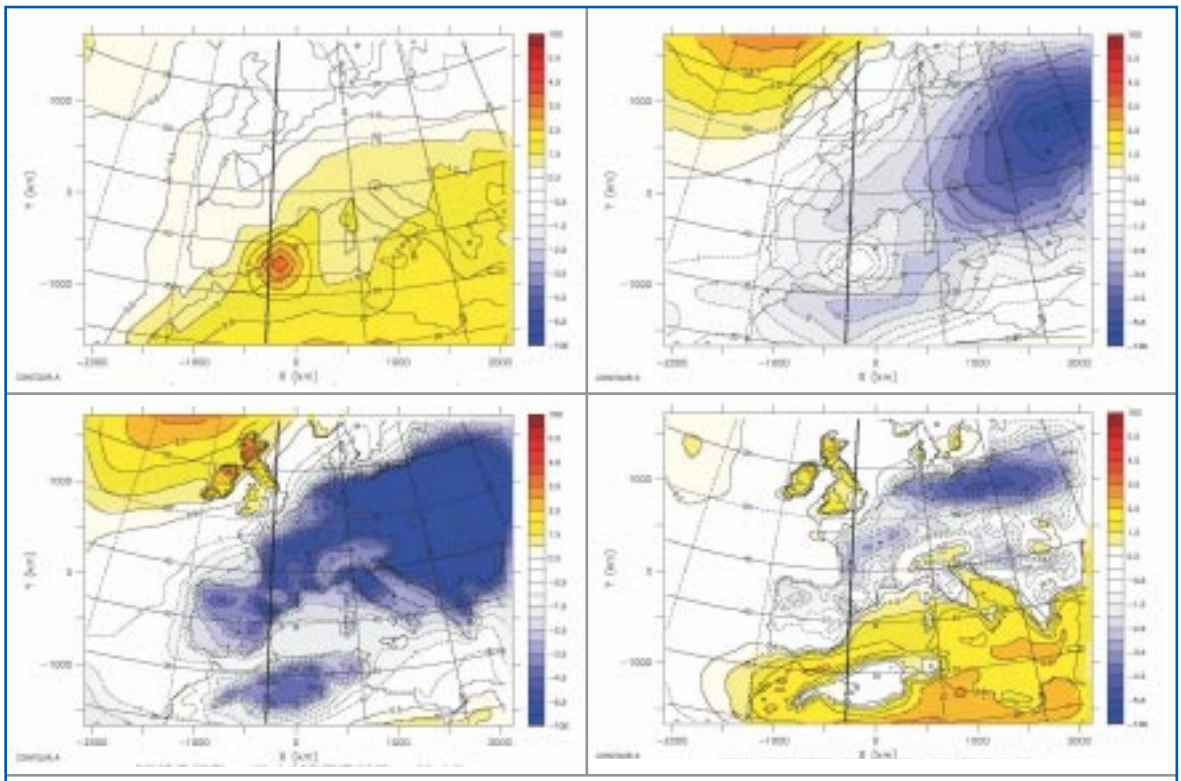

Figure 12a: *"B"– Baseline. Surface temperature DJF anomalies of experiments "B" minus control.*

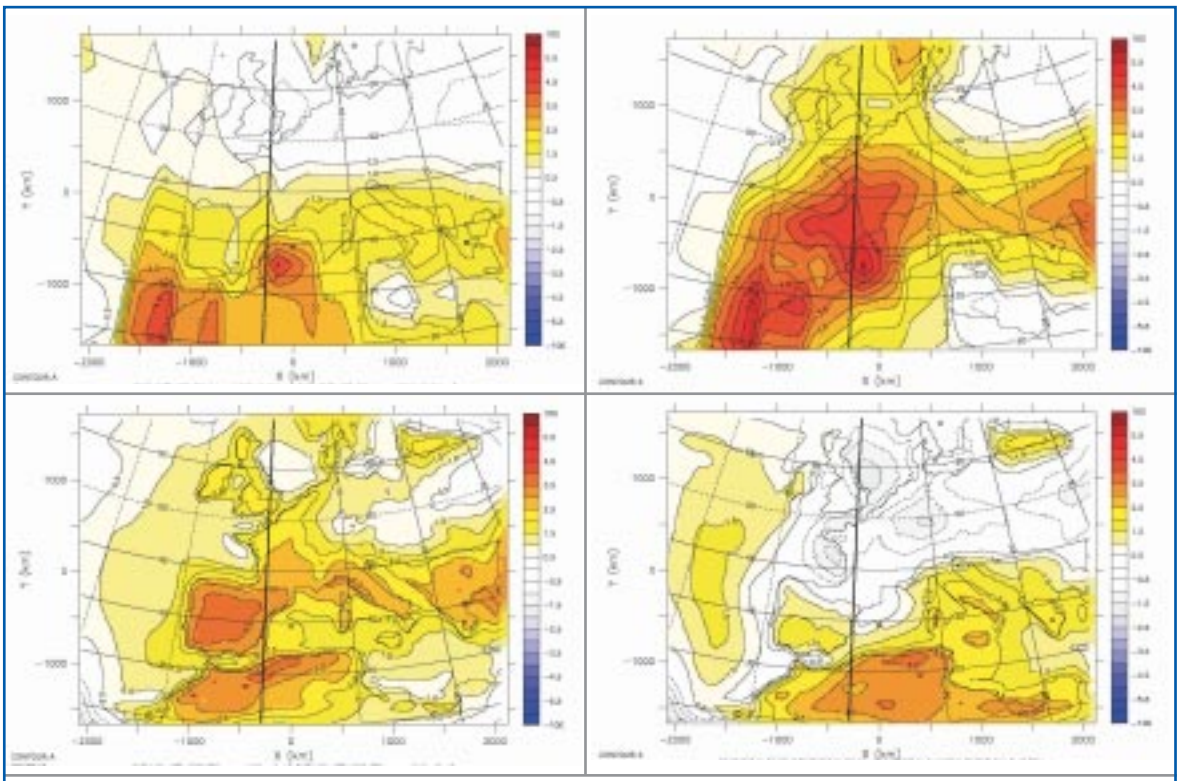

Figure 12b: *"B"– Baseline. Surface temperature JJA anomalies of experiments "B" minus control.*

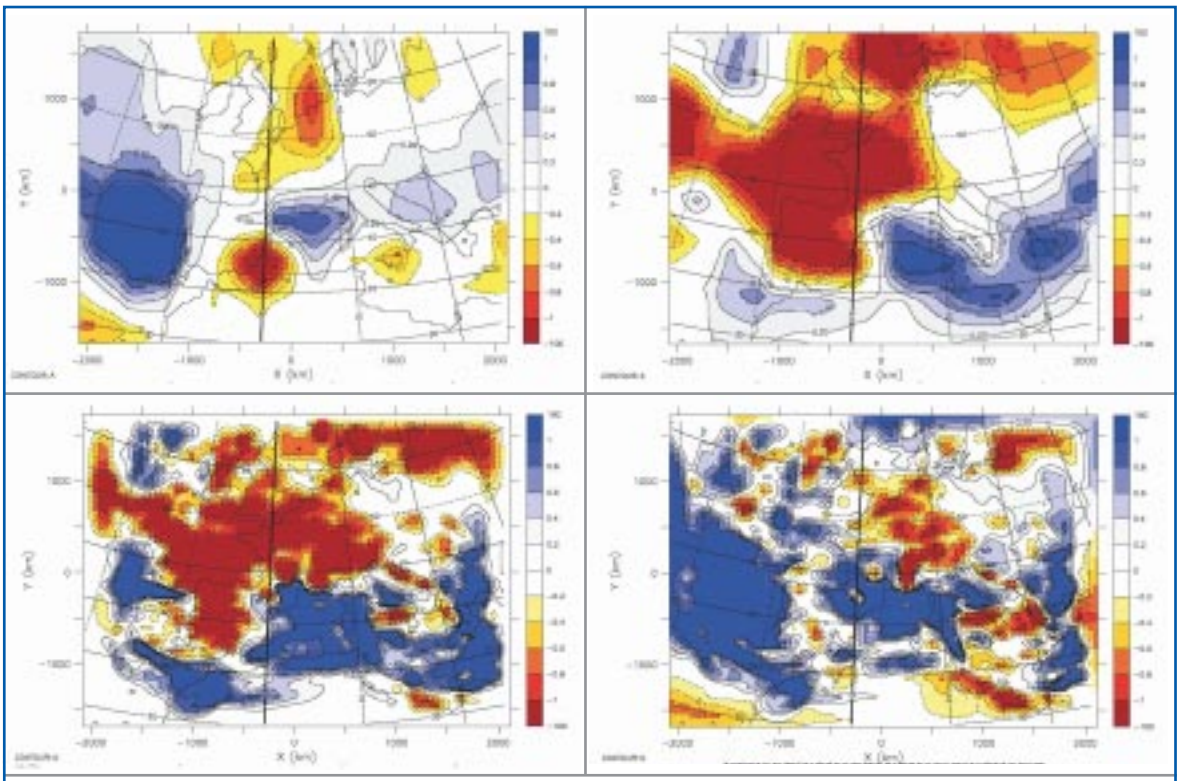

Figure 12c: *"B"– Baseline. Total precipitation DJF anomalies of experiments "B" minus control.*

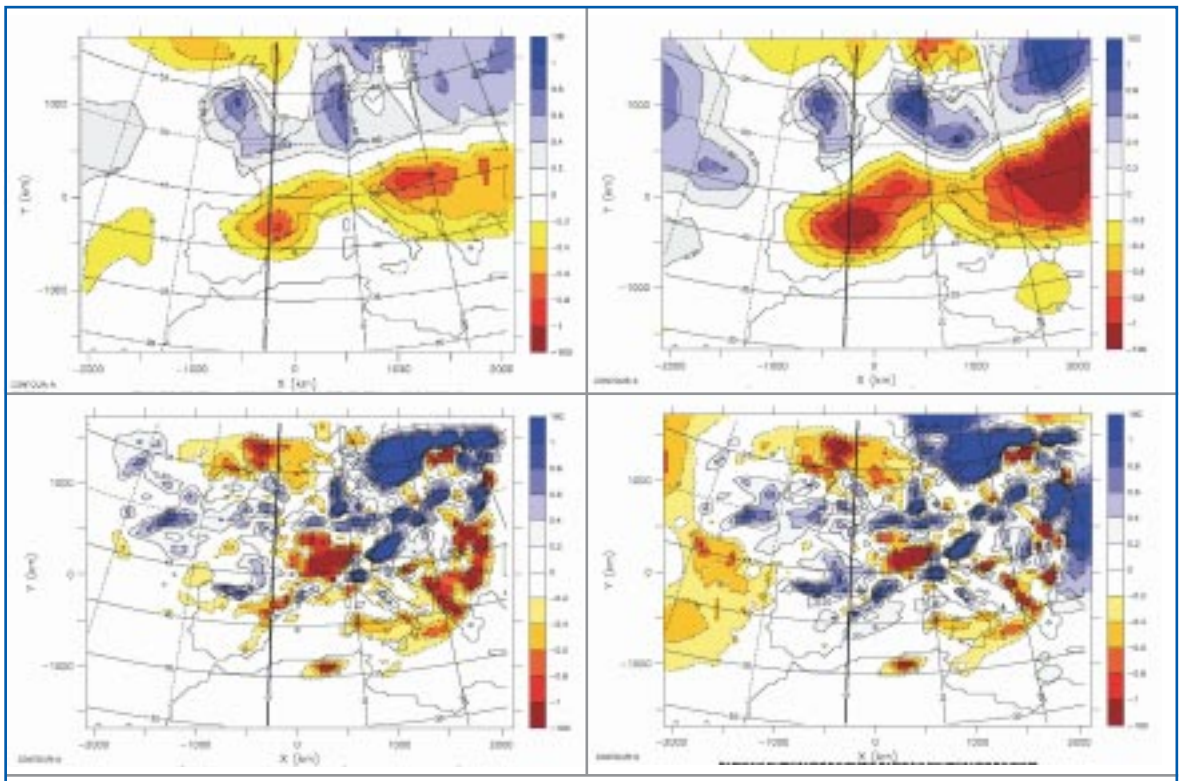

Figure 12d: *"B"– Baseline. Total precipitation JJA anomalies of experiments "B" minus control.*

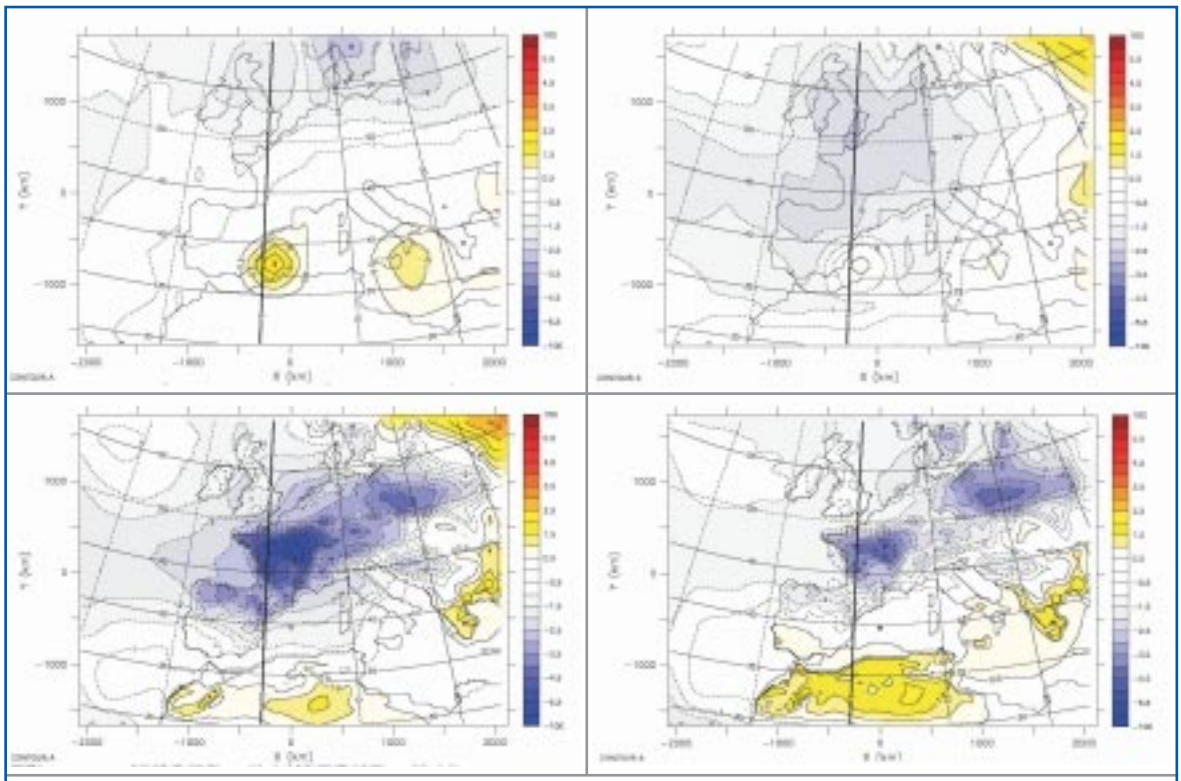

Figure 13a: *"F"– Baseline. Surface temperature DJF anomalies of experiments "F" minus control.*

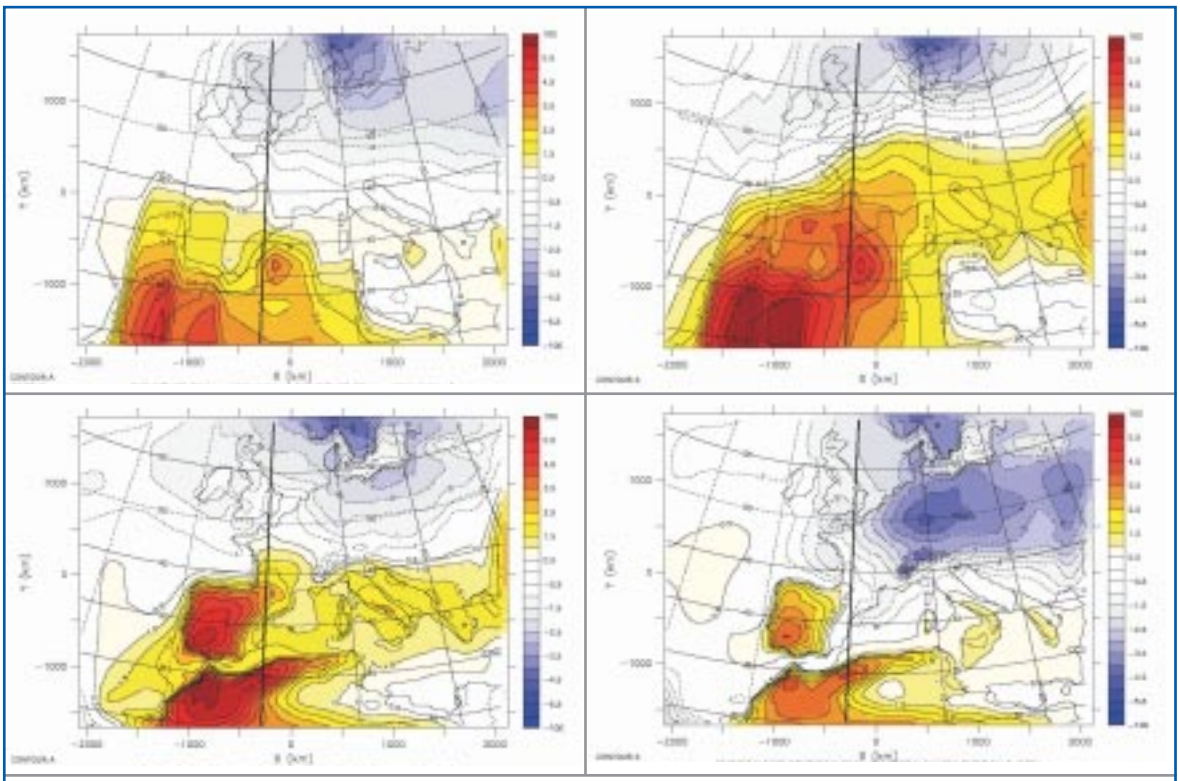

Figure 13b: *"F"– Baseline. Surface temperature JJA anomalies of experiments "F" minus control.*

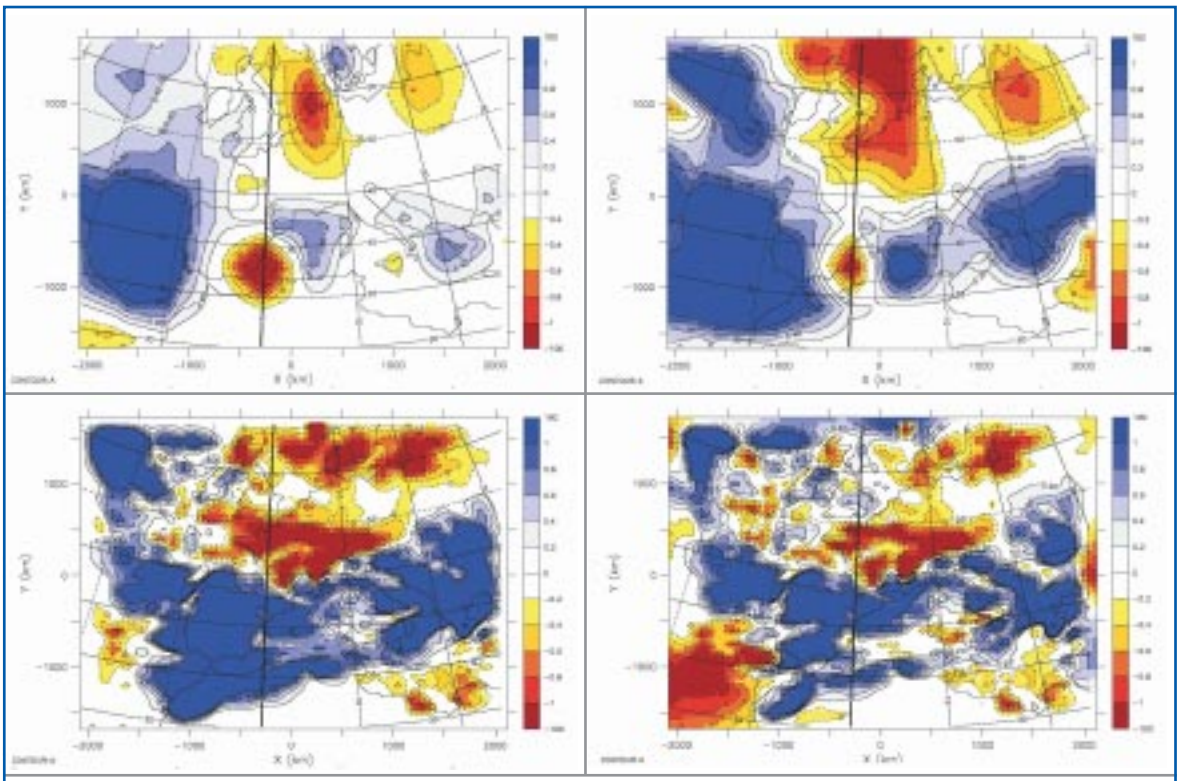

Figure 13c: *"F"– Baseline. Total precipitation DJF anomalies of experiments "F" minus control.*

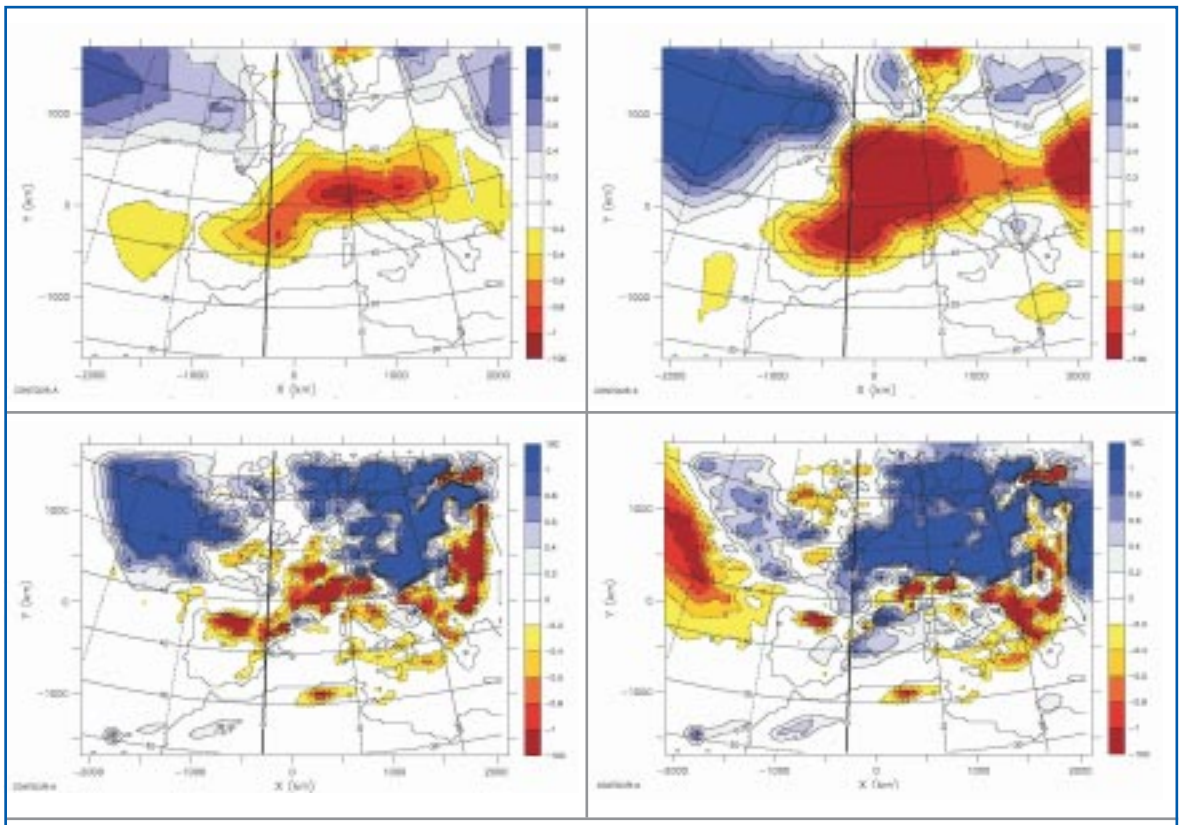

Figure 13d: *"F"– Baseline. Total precipitation JJA anomalies of experiments "F" minus control.*

Figure 14-20: *Monthly time series over the selected sites (see delimitation of the sites in text) for Central England, France, Spain, Germany and the Czech Republic, for the BIOCLIM simulations A to F and the control simulation.*

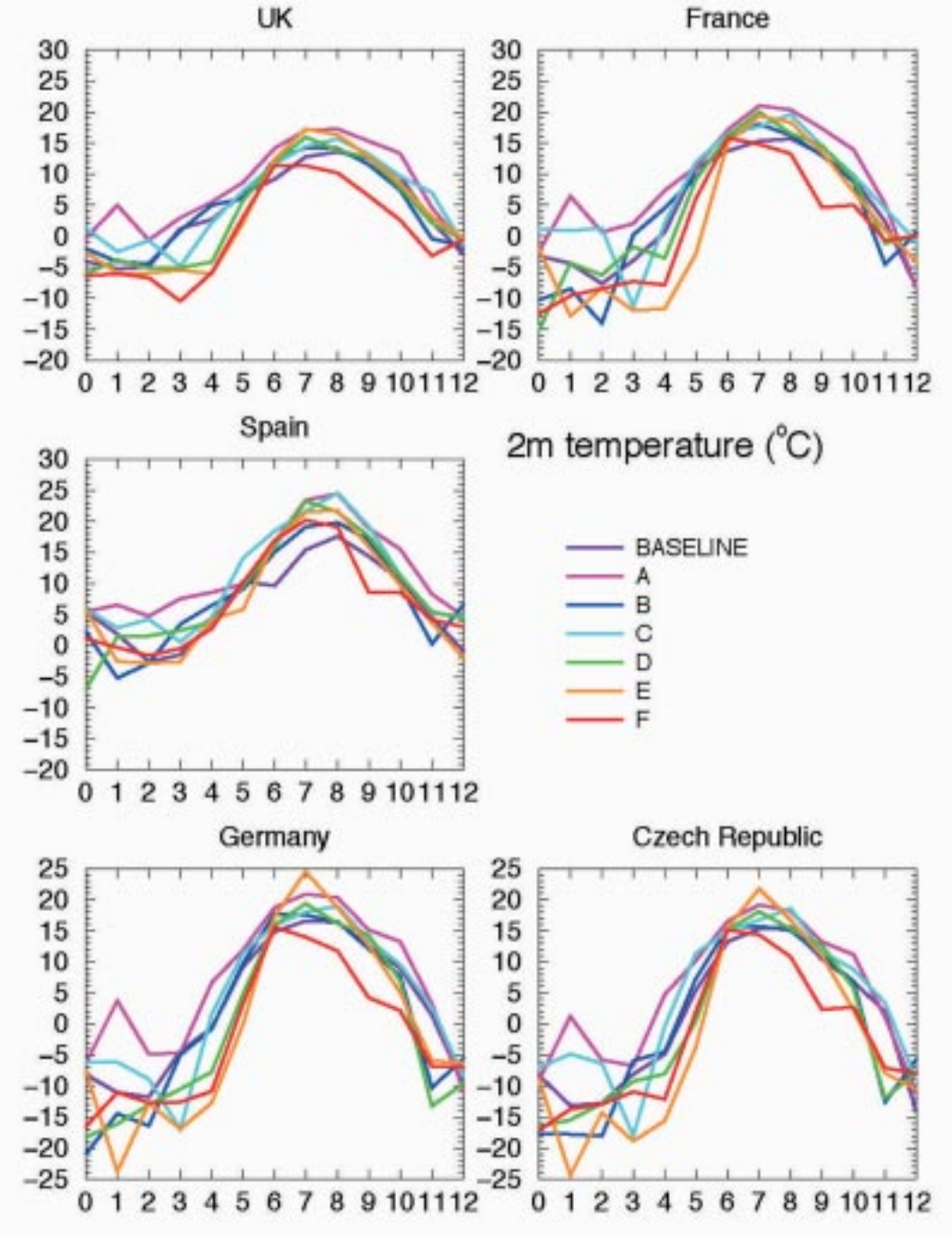

Figure 14: *2m temperature (°C)*

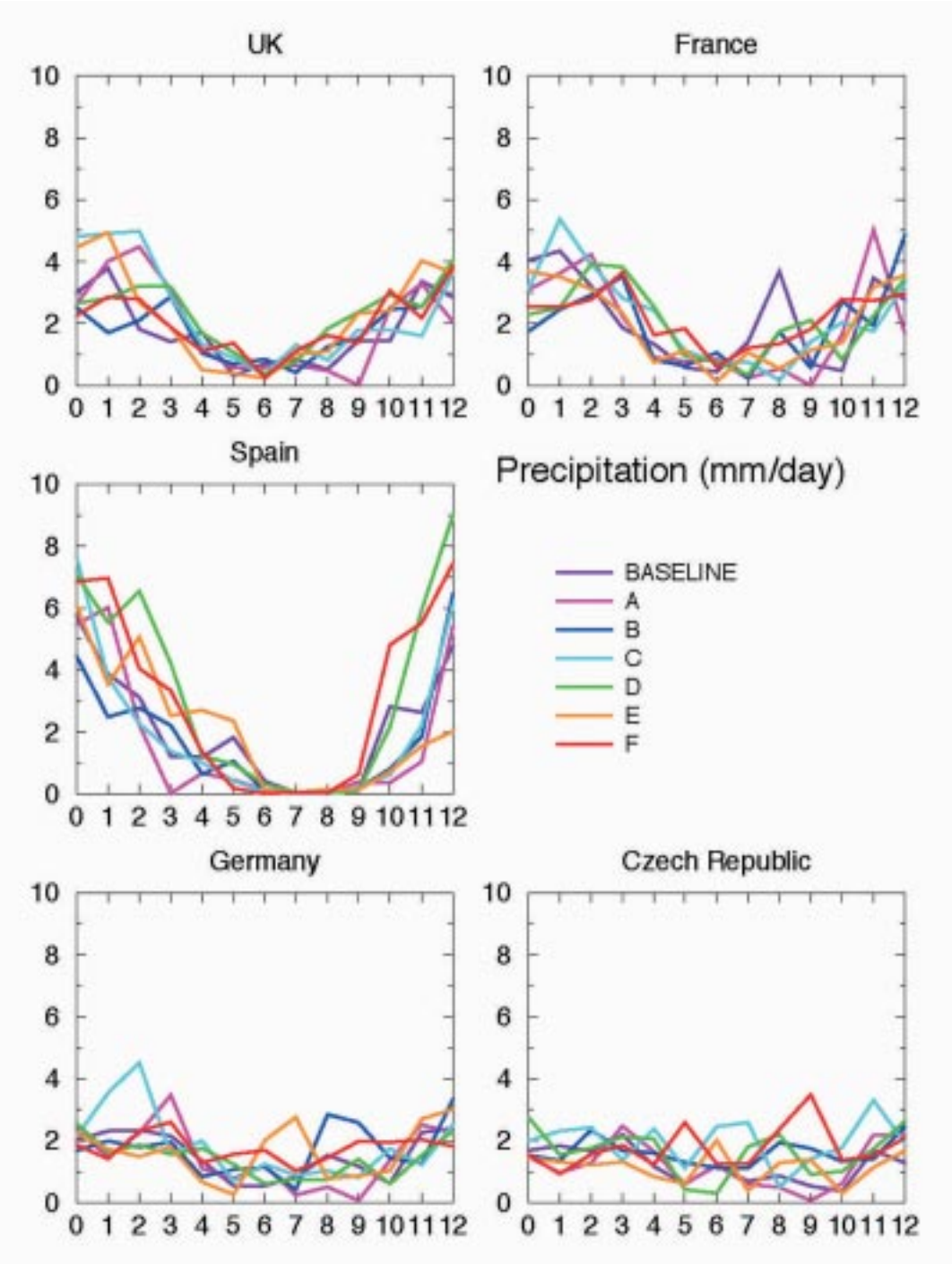

Figure 15: *Precipitation (mm.day^{-1})*

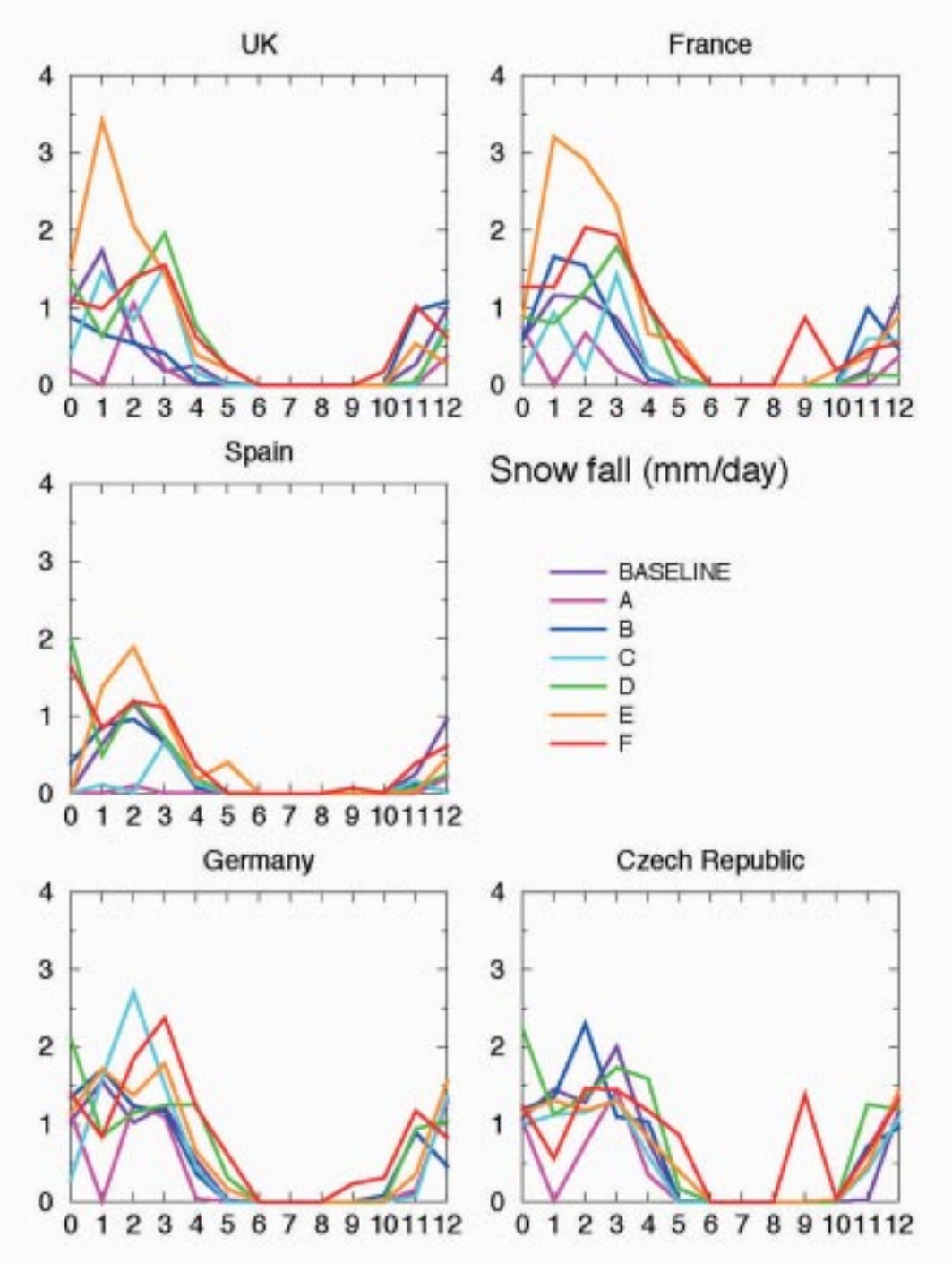

Figure 16: *Snow fall (mm.day^{-1})*

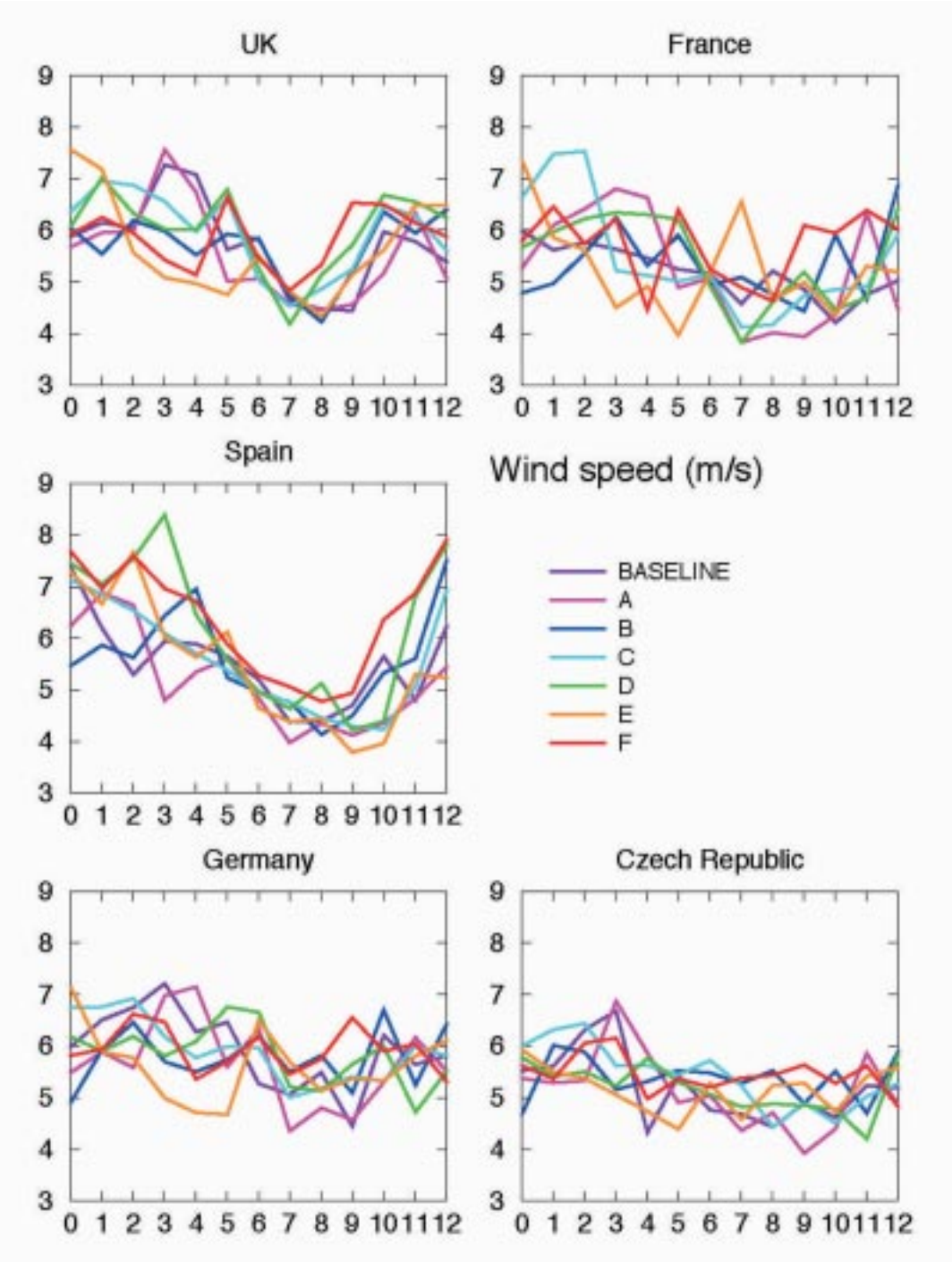

Figure 17: *Wind speed (m.s^{-1})*

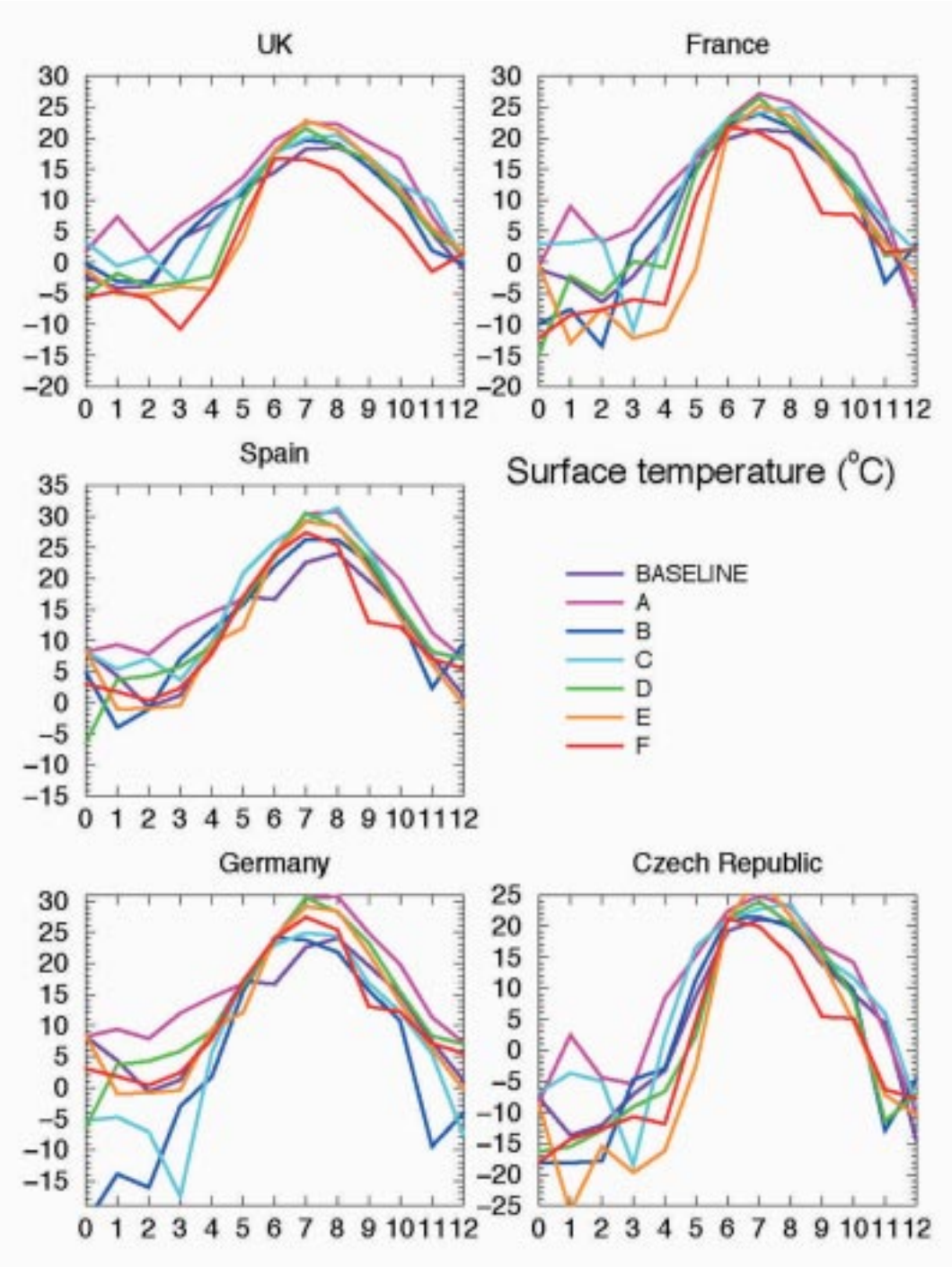

Figure 18: *Surface temperature (°C)*

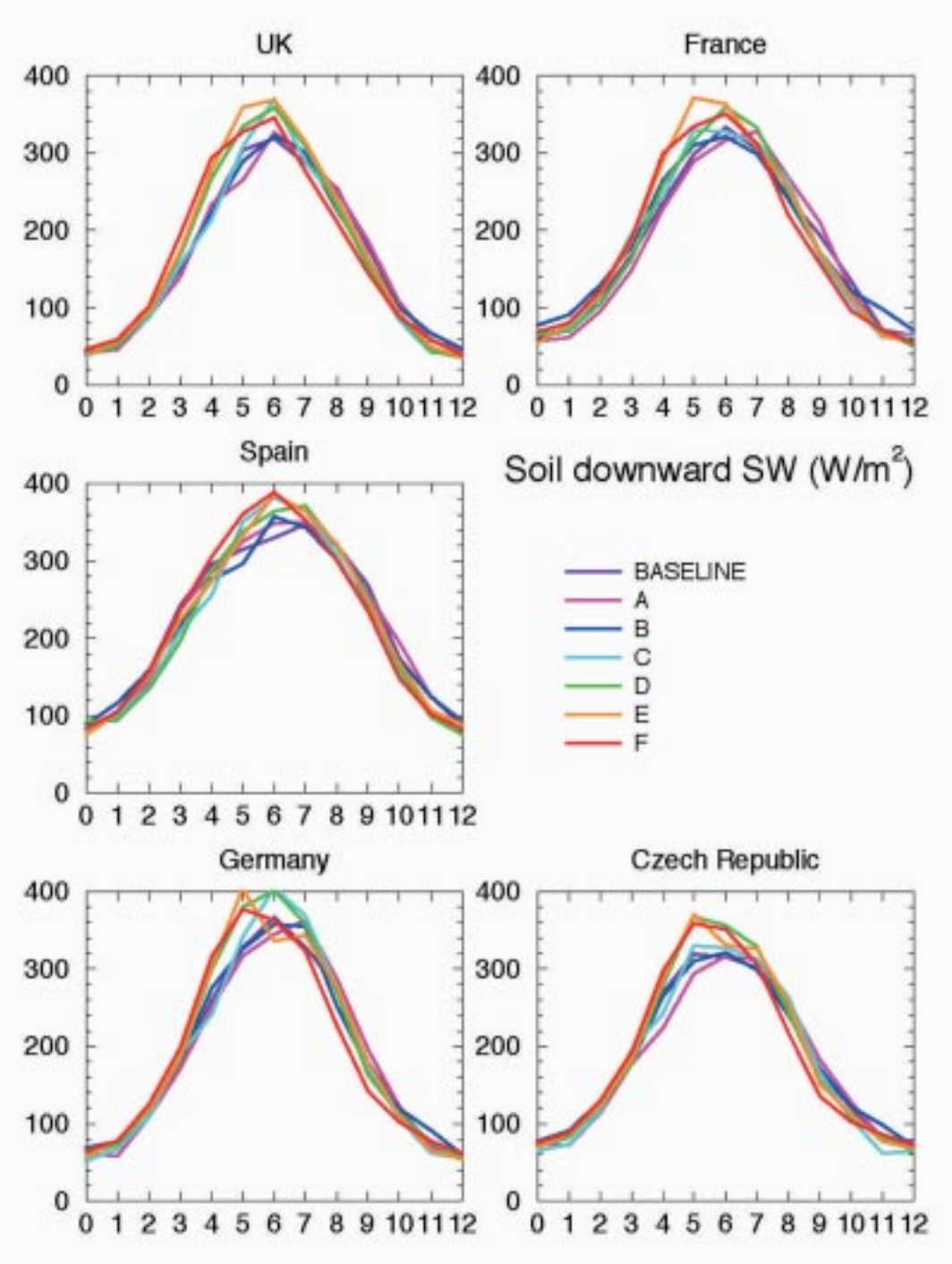

Figure 19: *Soil downward solar radiation (W.m^{-2})*

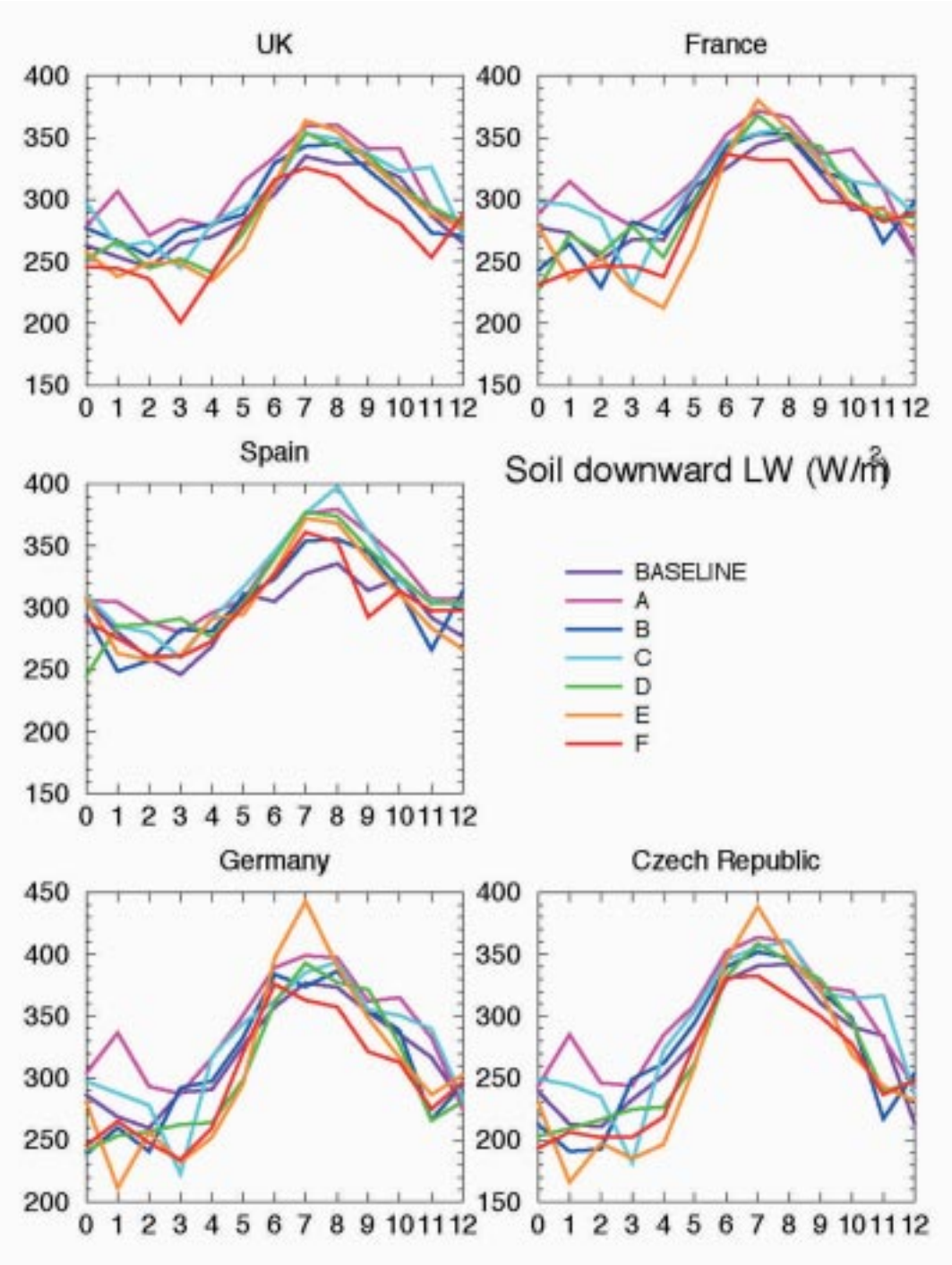

Figure 20: *Soil downward infrared radiation (W.m²)*


Bioclim

For further information contact:

BIOCLIM project co-ordinator, **Delphine Texier**

ANDRA, DS/MG (Direction Scientifique - Service Milieu Géologique

Parc de la Croix Blanche - 1/7, rue Jean-Monnet - 92298 Châtenay-Malabry Cedex - FRANCE
Tél.: +33 1 46 11 83 10
e-mail: delphine.texier@andra.fr
web site: www.andra.fr/bioclim/